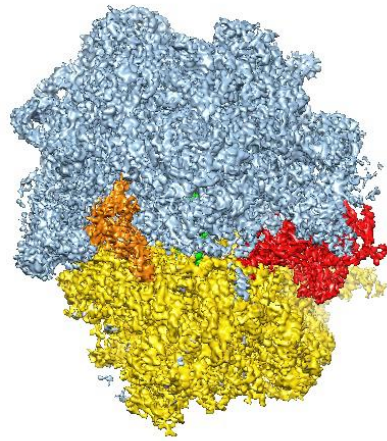


History of single-particle cryo-EM

Visualization of Biological Molecules in their Native States

NYSBC Cryo-EM course 2026



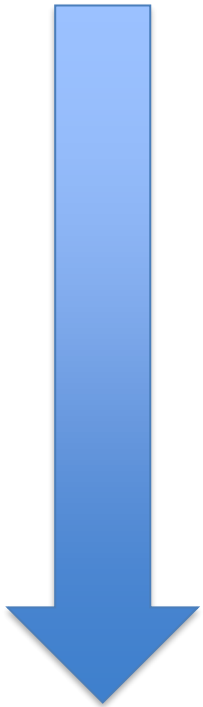
Joachim Frank

Department of Biochemistry and Molecular Biophysics

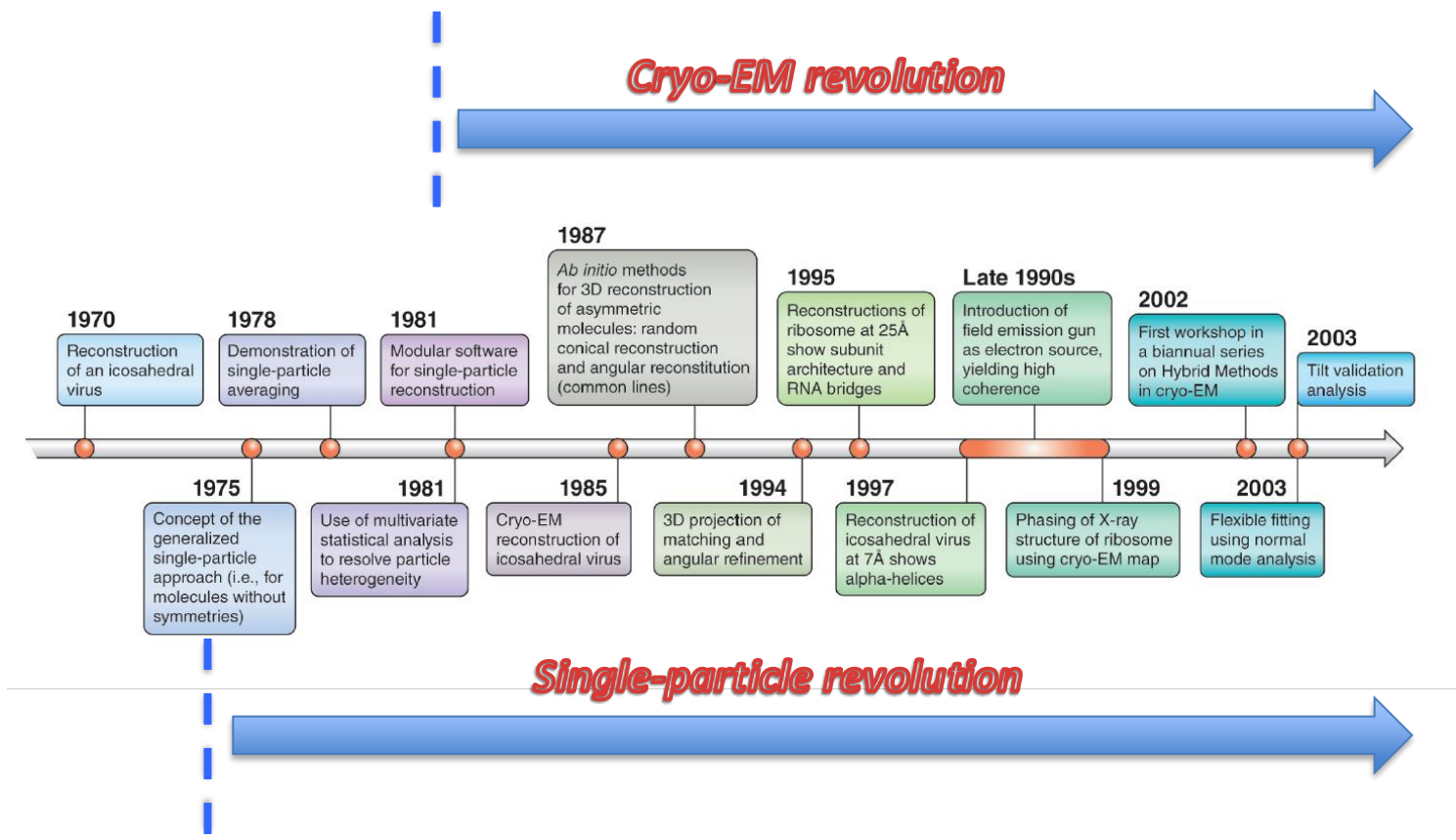
Department of Biological Sciences

Columbia University

Funding : National Institutes of Health

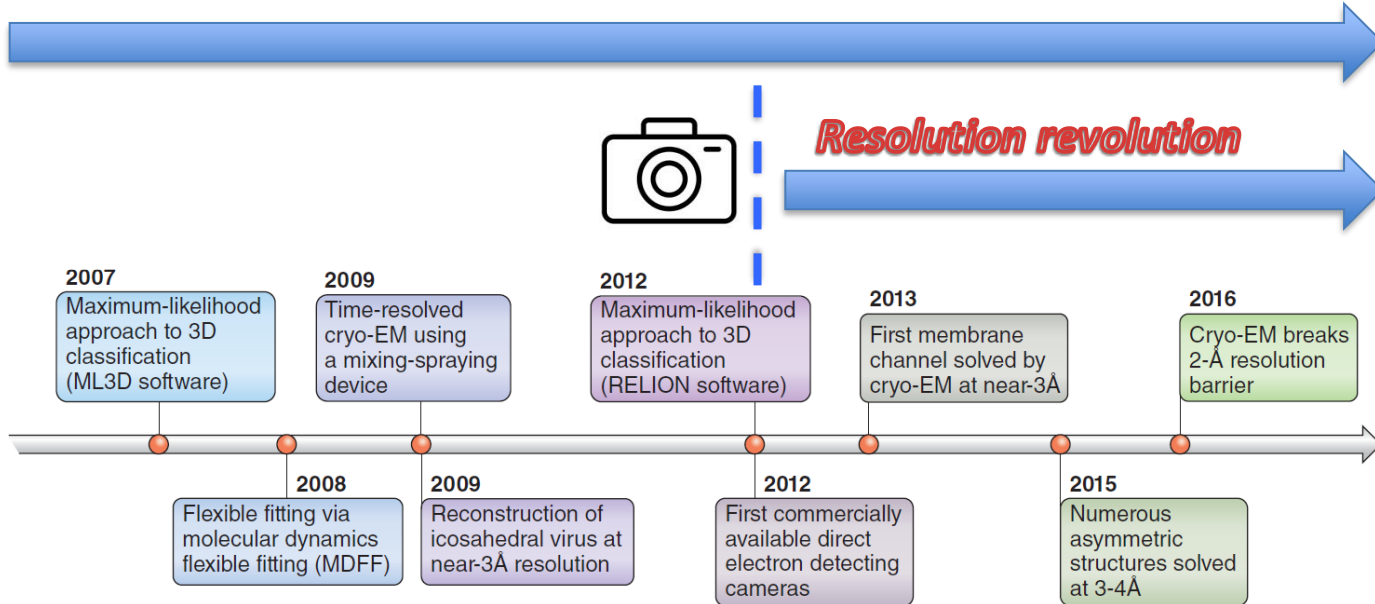


- Ancient history, EM and X-ray crystallography
- 1975 Single particle techniques -- the concept
- 1975 – 1987 development of SPIDER, programs for averaging, classification, 3D reconstruction
- 1981 Dubochet's discovery of vitreous ice
- 1987 First single-particle reconstruction – negative stain
- 1989 First single-particle reconstruction – vitreous ice
- 1990 – 2012 Cryo-EM reconstructions with increasing resolutions up to 5.5 Angstrom
- 2012 Direct electron detection cameras hit the market
- 2012 – now “resolution revolution”
- TODAY: exponential increase in cryo-EM structure depositions
- Future: Time-resolved cryo-EM & Mapping of continuum of states using cryo-EM



J. Frank, Nature Protocols 2017

Cryo-EM revolution



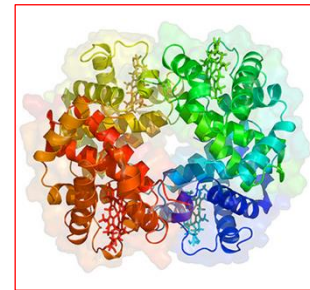
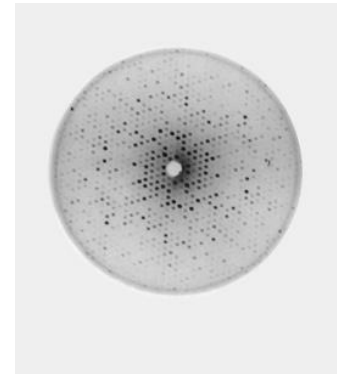
Single-particle revolution



J. Frank, Nature Protocols 2017

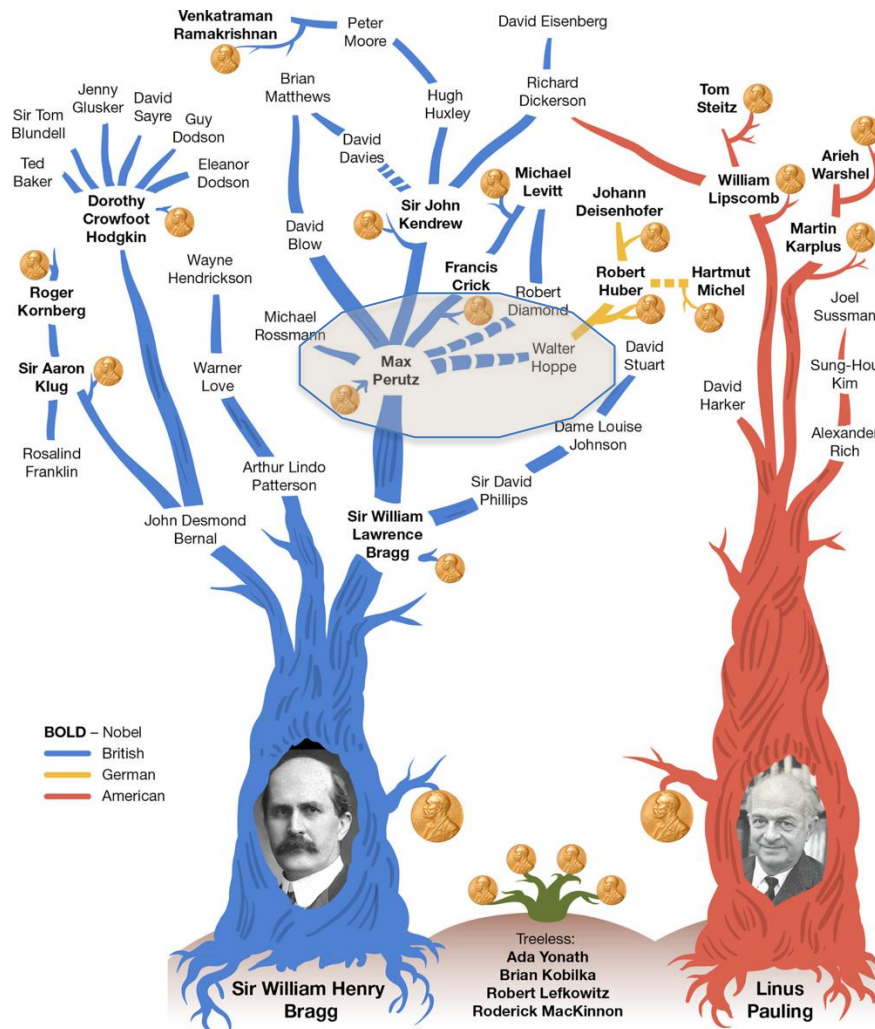
X-ray Crystallography

- Crystal: many copies of the molecule arranged in regular order.
- *Exposure to X-ray beam → diffraction pattern → structure determination.*
- X-ray beam must be high-intensity, crystal must be almost perfect.
- *To date ~ 140,000 structures solved by X-ray crystallography, available in public databanks.*
- **Crystal packing → molecules not visualized in all conformations/binding states that important for function.**
- ***Many molecules do not form highly ordered crystals.***
- **Sample quantity can be a big issue, as well.**
-



Max Perutz and John Kendrew with a model of hemoglobin, 1962

<http://www.mfpl.ac.at/vips/max-f-perutz/>



5% of all Nobel Prizes are related to X-ray crystallography. Half of these were for biomolecules

One of the first Hybrid Meetings!



Hirschegg, site of 1968 workshop on X-ray crystallography and EM of proteins organized by Walter Hoppe and Max Perutz.

Harold Erickson, Richard Henderson, Ken Holmes, Hugh Huxley, Nigel Unwin . . .



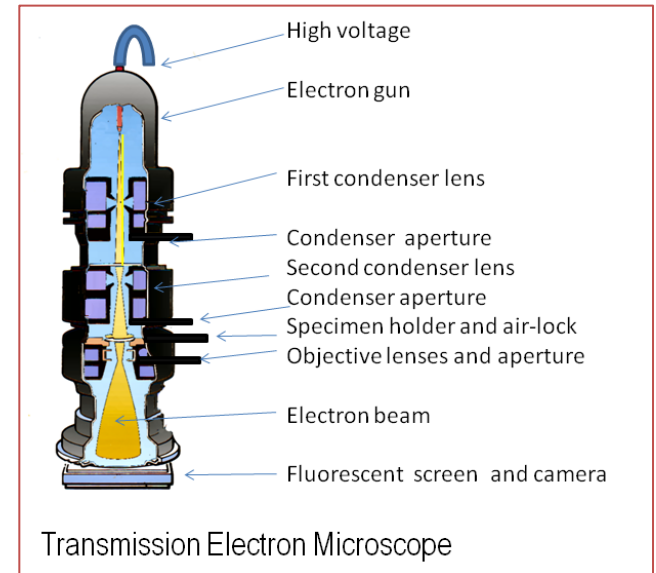
Conference site of the Hirschegg Meetings



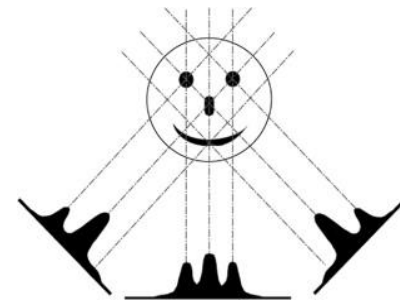
Walter Hoppe with Max Perutz in Hirschegg

Visualization/Structure Determination by Transmission Electron Microscopy

- The transmission electron microscope can be used to solve molecular structures.
- *Projection images formed at very high magnification, e.g. 30,000 x.*
- To reconstruct an object, many different views must be collected.
- ☹ *Sample must be very thin, electrons are readily absorbed by matter.*
- ☹ *Electrons strongly damage the molecules -- need for low dose! 10-20 electrons/square Angstrom.*
- ☹ *Images are very noisy (shot noise)*
- ☹ *Initially, negative staining needed to be used for sample preparation of molecules. Cryo-sample preparations were developed later.*
-



[http://www.newworldencyclopedia.org/entry/File:Electron Microscope.png](http://www.newworldencyclopedia.org/entry/File:Electron_Microscope.png)



LOW EXPOSURE 1971



ELSEVIER

Journal of Ultrastructure Research

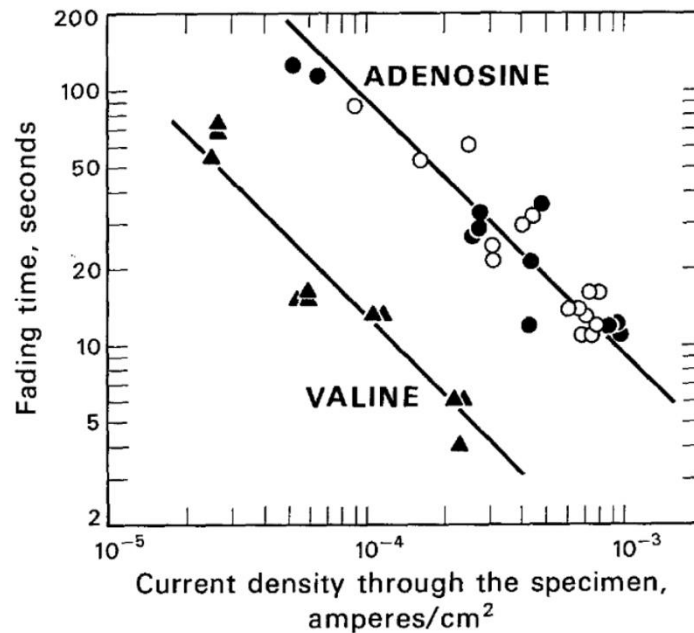
Volume 36, Issues 3-4, August 1971, Pages 466-482

Limitations to significant information
biological electron microscopy as a result of
radiation damage [1](#),

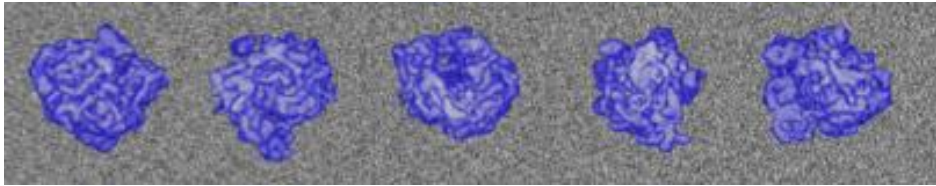
Robert M. Glaeser



Robert M. Glaeser



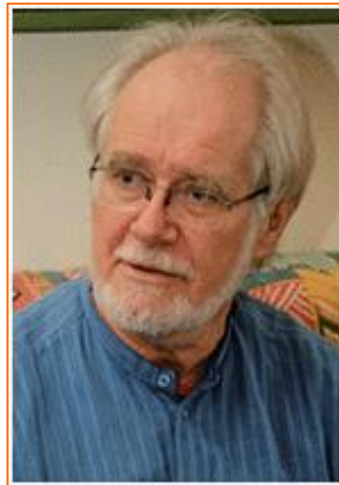
PLUNGE FREEZING/EMBEDDING IN VITREOUS ICE 1981



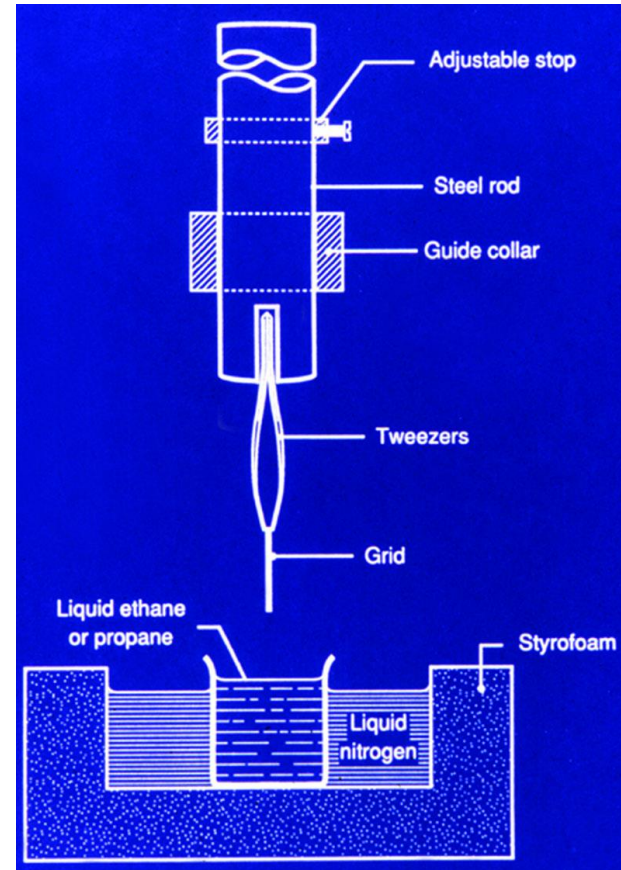
Molecules embedded in vitreous ice



Robert Glaeser
1976



Jacques Dubochet
1981



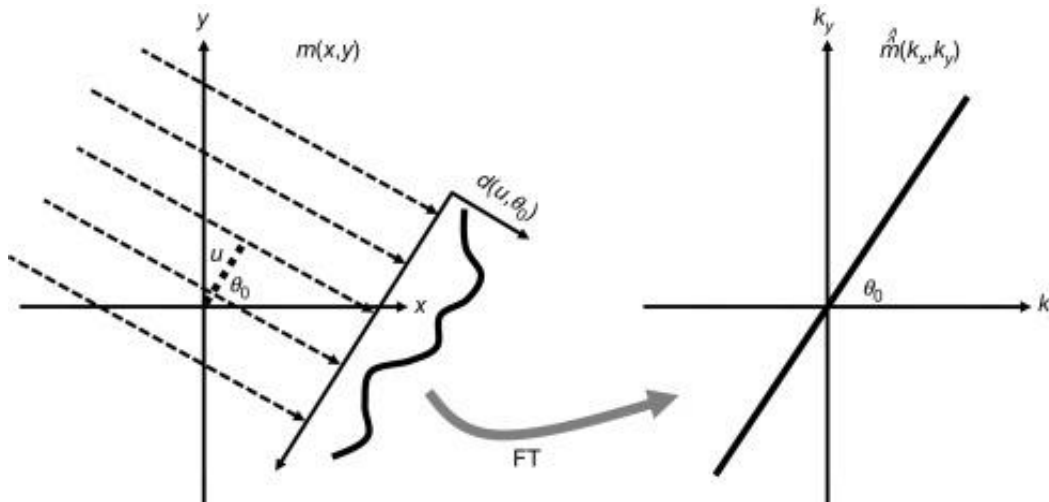
Plunge-freezer

3D RECONSTRUCTION

Among Radon's extensive work on calculus of variations, differential geometry and measure theory there is a paper appropriately titled

"Über die Bestimmung von Funktionen durch ihre Integralwerte längs gewisser Mannigfaltigkeiten." (1905)

It describes the way a multidimensional function is related to its projections, both in real and Fourier space.

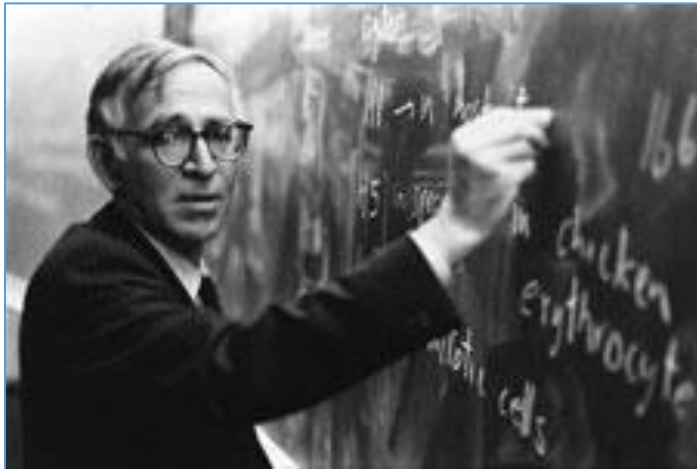


Johannes Radon
1887 - 1956

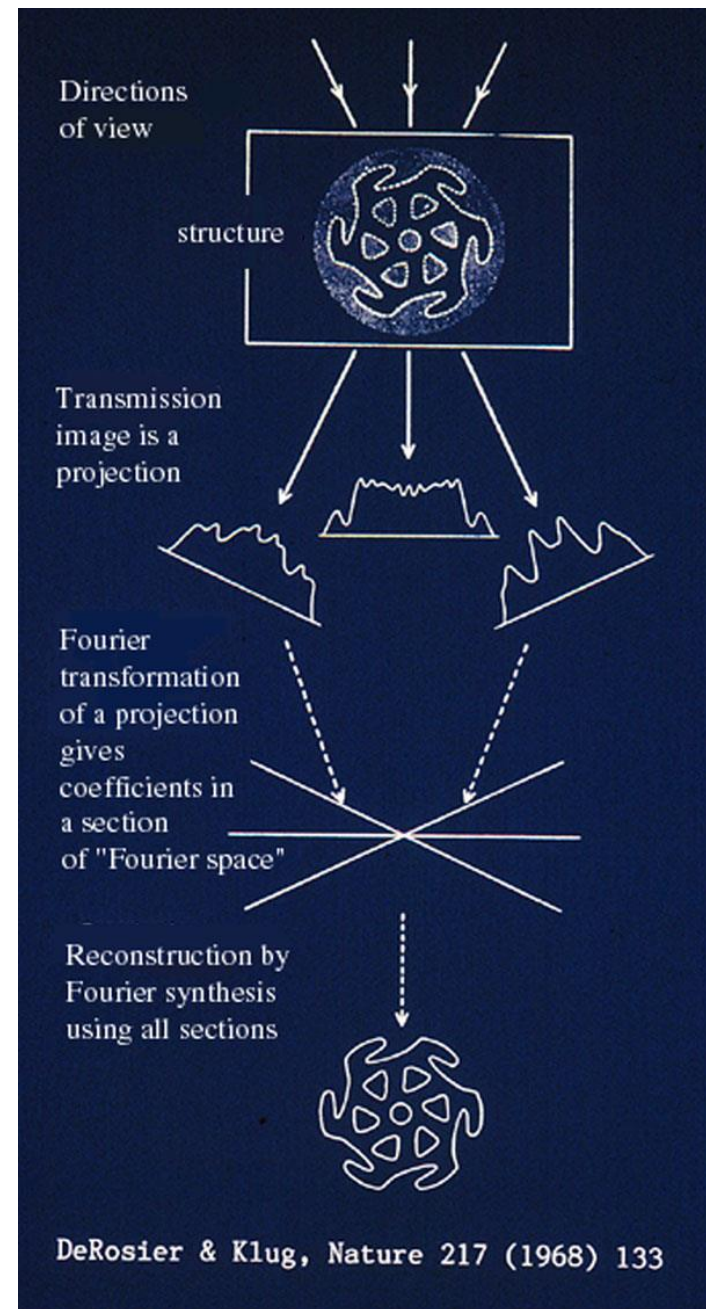
THREE-DIMENSIONAL RECONSTRUCTION:
STRUCTURES WITH HELICAL SYMMETRY. 1968
(sample prep: negative staining)

Pioneering work: 3D reconstruction of a
bacteriophage tail using the Fourier-Bessel
approach, 1968

Application of the Projection-Slice Theorem

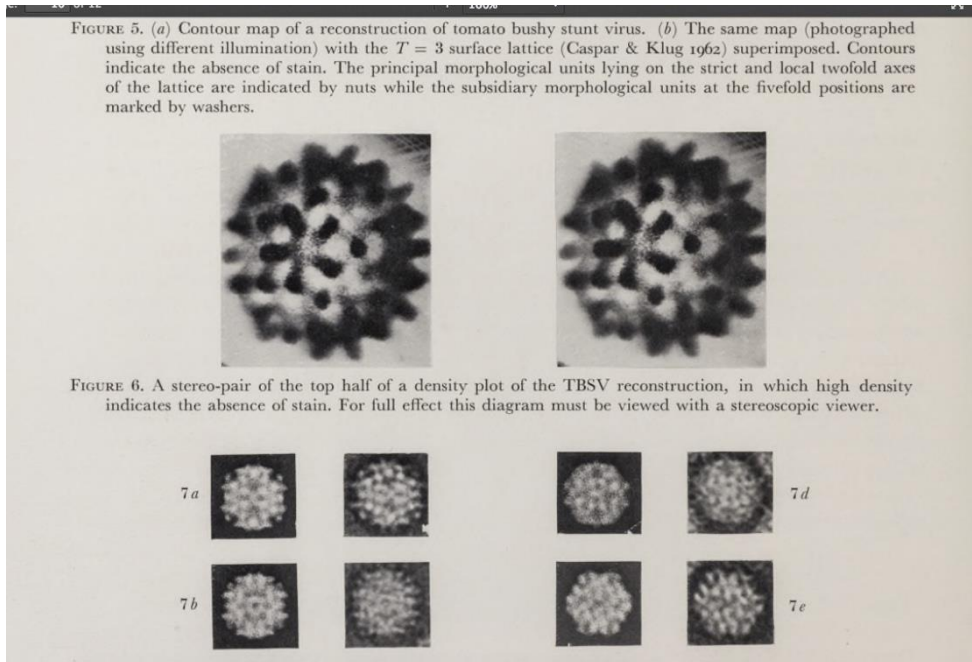


Aaron Klug and David DeRosier, LMB/MRC Cambridge



THREE-DIMENSIONAL RECONSTRUCTION: VIRUSES WITH ICOSAHEDRAL SYMMETRY (sample prep: negative staining) 1970

tomato bushy stunt virus



Tony Crowther

R. A. Crowther, Phil. Trans. Roy. Soc. 1971

THREE-DIMENSIONAL RECONSTRUCTION: STRUCTURES THAT FORM 2D CRYSTALS (glucose embedding). 1975

(Reprinted from Nature, Vol. 257, No. 5521, pp. 28-32, September 4, 1975)

Three-dimensional model of purple membrane obtained by electron microscopy

R. Henderson & P. N. T. Unwin

MRC Laboratory of Molecular Biology, Hills Road, Cambridge CB2 2QH, UK

A 7-Å resolution map of the purple membrane has been obtained by electron microscopy of tilted, unstained specimens. The protein in the membrane contains seven, closely packed, α -helical segments which extend roughly perpendicular to the plane of the membrane for most of its width. Lipid bilayer regions fill the spaces between the protein molecules.

The purple membrane is a specialised part of the cell membrane of *Halobacterium halobium*¹. Oesterhelt and Stoekenius² have shown that it functions *in vivo* as a light-driven hydrogen ion pump involved in photosynthesis. It contains identical protein molecules of molecular weight 26,000, which make up 75% of the total mass, and lipid which makes up the remaining 25% (ref. 3). Retinal, covalently linked to each protein molecule in a 1:1 ratio is responsible for the characteristic purple colour³. These components together form an extremely regular two-dimensional array⁴.

We have studied the purple membrane by electron microscopy using a method for determining the projected structures of unstained crystalline specimens⁵. By applying the method to tilted specimens, and using the principles put forward by De Rosier and Klug⁶ for the combination of such two-dimensional views, we have obtained a three-dimensional map of the membrane at 7 Å resolution. The map reveals the location of the protein and lipid components, the arrangement of the polypeptide chains within each protein molecule, and the relationship of the protein molecules in the lattice.

Electron microscopy and diffraction

The purple membrane was prepared under normal conditions from cultures of *H. halobium*³ and applied to the microscope grid in the presence of 0.5% glucose. The purified membranes are mostly oval sheets up to 1.0 μ m in diameter and about 45 Å thick^{3,7}. The array of molecules making up these sheets is accurately described⁸ as an almost perfect crystal of space group P3 ($a = 62$ Å) with a thickness of one unit cell only in the direction of the c axis. A single membrane thus contains up to 40,000 unit cells; that is 120,000 protein molecules (three per unit cell).

These large periodic arrays from which electron diffraction patterns and defocused bright field micrographs are recorded⁹ enable us to overcome the principal problem normally associated with high resolution electron microscopy of unstained biological materials; that is, sensitivity to electron damage¹⁰. Only a small number of electrons can pass through each unit cell before it is destroyed, but because of the large number of unit cells, the information in the diffraction patterns and micrographs is sufficient to provide a picture of the average unit cell. The micrographs recorded with such low doses of electrons appear featureless, since the statistical fluctuation in the number of electrons striking the plate is large compared with the weak phase contrast (<1%) produced by defocusing.

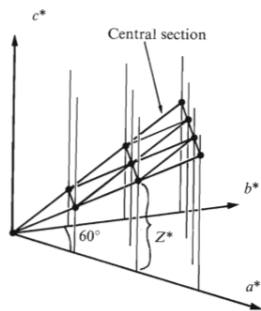
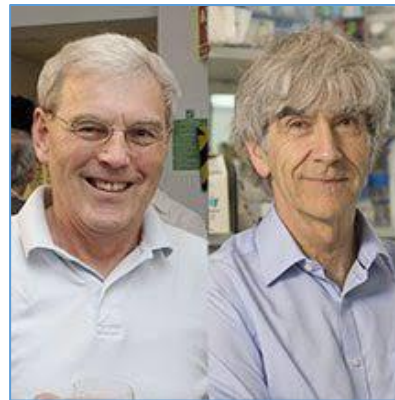


Fig. 1 Part of the three-dimensional reciprocal lattice showing the geometry of the lattice lines in the hexagonal space group P3. a^* , b^* and c^* are the reciprocal lattice vectors. a^* and b^* lie in, and c^* is perpendicular to the plane of the membrane. A central section which is perpendicular to the incident electron beam has been drawn through the lattice. The intersection of this central section with the reciprocal lattice is determined by the angle of tilt and the axis about which the membrane is tilted. Individual diffraction patterns and micrographs provide the amplitudes and phases in this section at the points shown. z^* represents the coordinate along the c^* direction of one of the points. The angle of tilt was measured to within 2° for each of the specially modified, tilted specimen holders, and the direction of the tilt axis on the photographic plate was established during operation of the microscope. However, estimates based on the geometry of the spacings of the lattice points (for high tilt angles), the variation of the degree of underfocus across the plate (for low tilt angles), and least squares refinement against data obtained at high tilt angles (for diffraction patterns) provided more accurate figures which were used in the calculation. The accuracy of measurement of both the amplitudes and phases depended on having sharp lattice lines. We therefore took care to ensure that, on the microscope grid, the membranes remained coherently ordered and flat to within $1/5^\circ$.

As a result, analysis of each micrograph by densitometry and computer processing¹¹ is required to combine the information from individual unit cells.

Solution of the three-dimensional structure of the purple membrane requires the determination of the amplitudes and phases in three dimensions of the Fourier terms into which it can be analysed. The diffraction pattern or Fourier transform of the membrane is not a three-dimensional lattice of points as is the case with a normal crystal, but since it is only one unit cell thick, a two-dimensional lattice of lines which are continuous in the direction of c^* (that is perpendicular to the membrane). A single electron diffraction experiment therefore

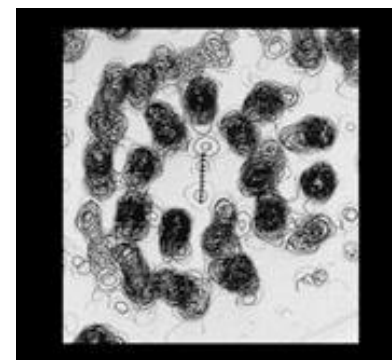
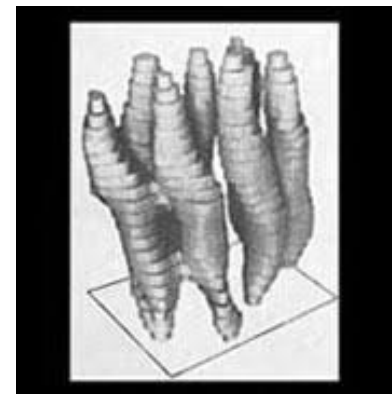


Richard Henderson
and Nigel Unwin

Purple membrane
Protein

Bacteriorhodopsin

Electron dose is spread
over many repeats
of the molecule in the
crystal



First EM of molecular structures focused on crystalline arrangements:

helical, planar 2-D, icosahedral

averaging over many repeats of the molecule was implicit in the Fourier-based data processing

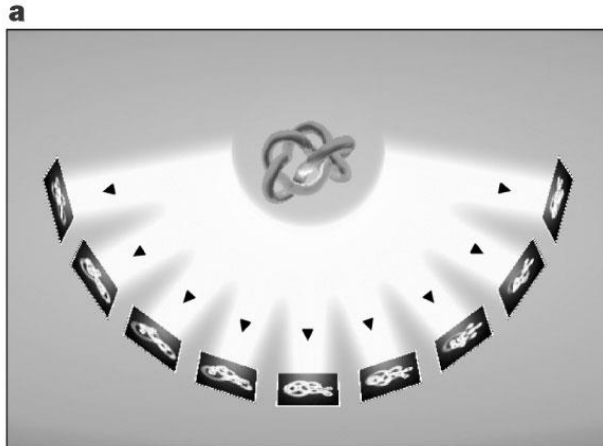
each symmetry involved a different math/computational approach

What about molecules not bound in a crystal?

What about molecules without symmetry?

Why Crystals?

3D Reconstruction of Asymmetrical Molecules by Electron Tomography ~1968



- Electron Tomography of single molecules
- Examples: fatty acid synthetase and ribosome
- **BUT: Accumulated electron exposure exceeded 1000 e^-/A^2**



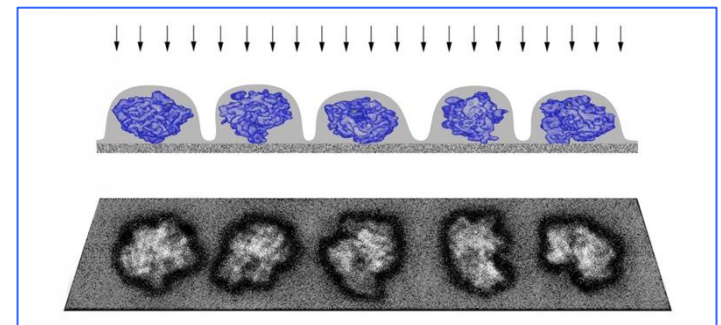
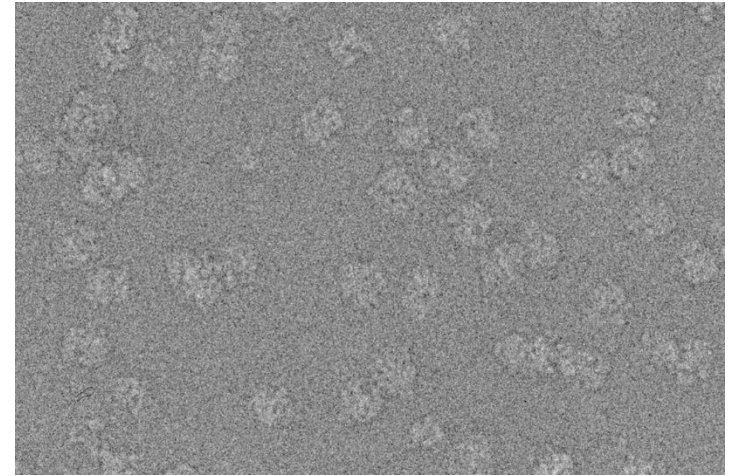
Walter Hoppe

(MPG Archive)

Why Crystals?

3D Reconstruction of Asymmetrical Molecules by Single-Particle Techniques – the Concept 1975

- Single-particle techniques: structural information from images of single (i.e., unattached) molecules in many copies.
- *Molecules are free to assume all naturally occurring conformations.*
- Molecules are randomly oriented.
- *A single snapshot may already give us hundreds of particle views.*
- As we collect more snapshots, more orientations will be covered, until we have enough for reconstructing the molecule in three dimensions.
-



EM images can be aligned to within better than 3 Angstrom!

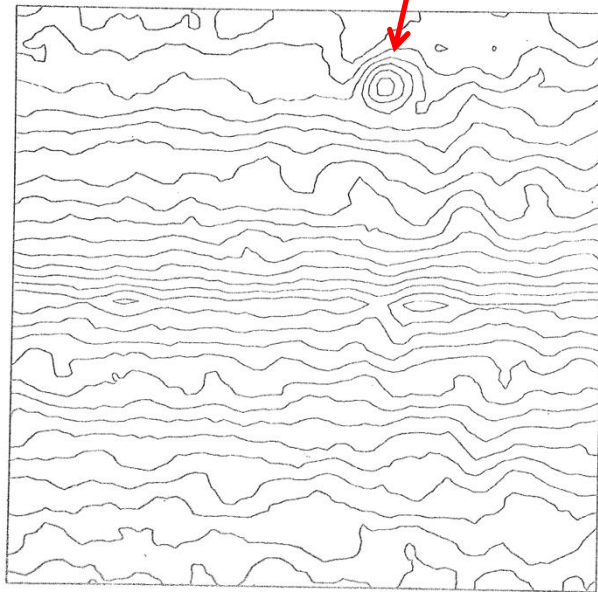


Abb. 11a,b Graphitfolie; Korrelationsfunktionen großer Teilbereich). Höhenschichtlinien:
 a) Abstand 0.006, von 0.0 bis 0.03
 b) Abstand 0.001, von 0.147 bis 0.166

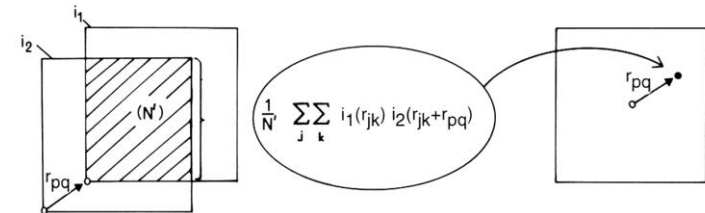


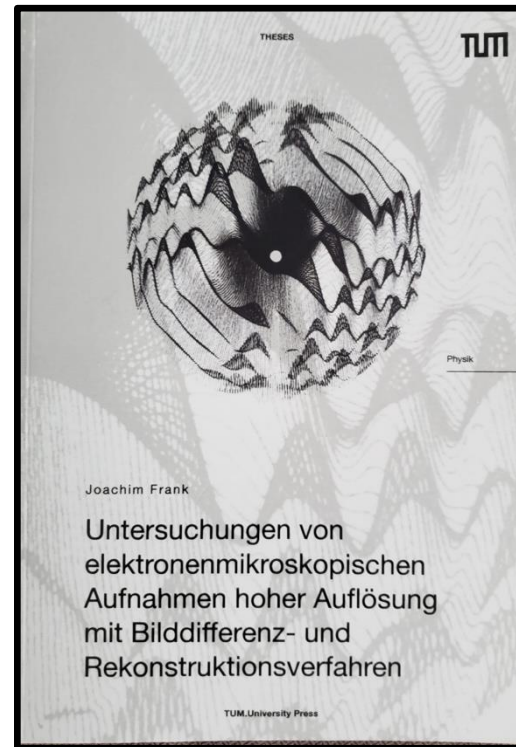
Fig. 3.8. Definition of the cross-correlation function. Image 1 is shifted with respect to image 2 by vector r_{pq} . In this shifted position, the scalar product of the two images arrays is formed and put into the CCF matrix at position (p, q) . The vector r_{pq} is now allowed to assume all positions on the sampling grid. In the end, the CCF matrix has an entry in each position. From Frank (1980). Reproduced with permission of Springer-Verlag, New York.

Cross-correlation function of 2 successive micrographs of the same carbon film

J. Frank, Ph.D. thesis 1970

Dissertation at
Technical University Munich,
published in 2019,
49 years after completion

Image on the cover:
Young's fringes



J. Frank (1970) "Analysis of high-resolution electron micrographs using image difference and reconstruction methods"

SHORT NOTE

AVERAGING OF LOW EXPOSURE ELECTRON MICROGRAPHS OF NON-PERIODIC OBJECTS

Joachim FRANK *

The Cavendish Laboratory, Free School Lane, Cambridge CB2 3RQ, UK

Received 20 October 1975

The investigation concerns the possibility of extending to non-periodic objects the low exposure averaging techniques recently proposed for non-destructive electron microscopy of periodic biological objects. Two methods are discussed which are based on cross-correlation and are in principle suited for solving this problem.

1. Introduction .

Recent work on low exposure techniques combined with averaging [1–3] (called ‘SNAP shot techniques’ in [3]) shows that information can be retrieved from periodic biological objects at higher than conventionally available resolutions [4]. Unwin and Henderson [2] were able to achieve 7 Å image resolution, by re-

6]. In these applications, the contrast of the individual marker atom image to be superposed is sufficient for straightforward alignment. However, the requirement of subminimum exposure poses a new problem: the alignment of features that are only faintly visible on a noisy background.

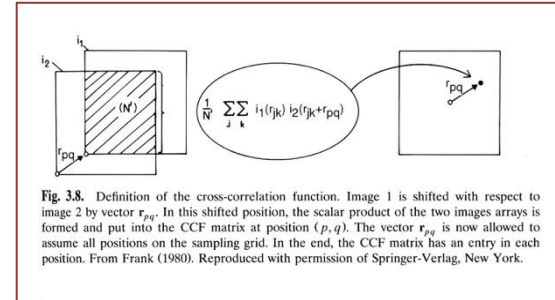
Conditions for effective cross-correlation alignment of
two images of a molecule (size D)

$$D \geq \frac{3}{c^2 dp_{crit}}$$

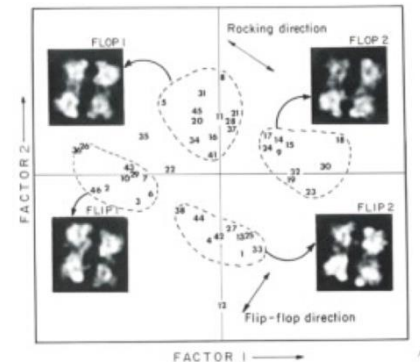
PARTICLE SIZE > 3 / [CONTRAST² x RESOLUTION (in Å) x CRITICAL ELECTRON DOSE]

Saxton & Frank, Ultramicroscopy 1977

Devil in the detail – *Problems to be solved:*



- ALIGN IMAGES
- CTF CORRECTION
- SORT/CLASSIFY IMAGES
- FIND PROJECTION ANGLES
- RECONSTRUCT IN 3D



SPIDER -- Modular image processing program

Toronto EM conference abstract 1978

Ultramicroscopy 1981

Some of the operations
(out of hundreds):

AC -- autocorrelation

CC -- cross-correlate 2 images

FT -- Fourier transform

RT -- rotate

SH -- shift

WI -- window



“WORKBENCH” FOR PROCESSING IMAGES

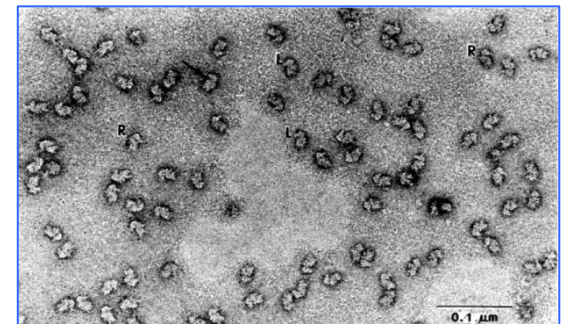
The Ribosome – its role in the development of Single-Particle Techniques



1927 - 1994

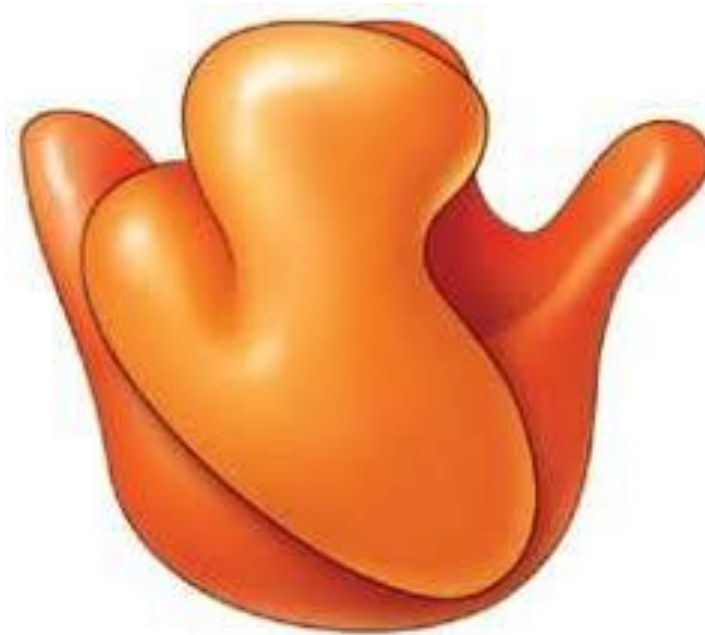
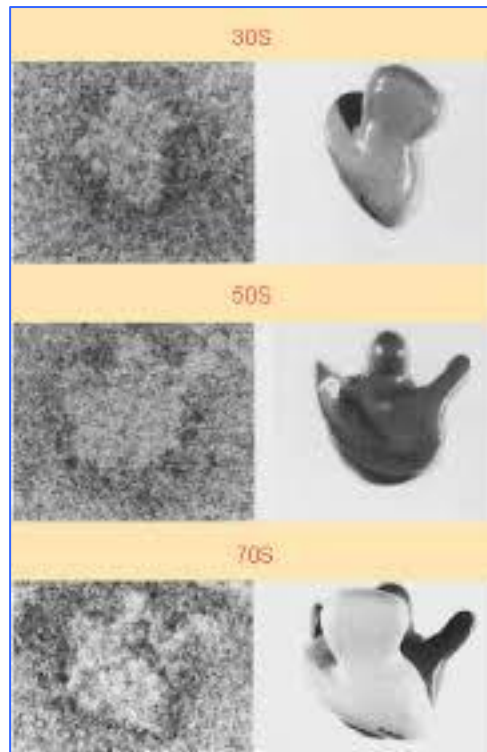
- Large size
- Sturdy
- High contrast

Miloslav Boublik
Roche Institute, Nutley, NJ





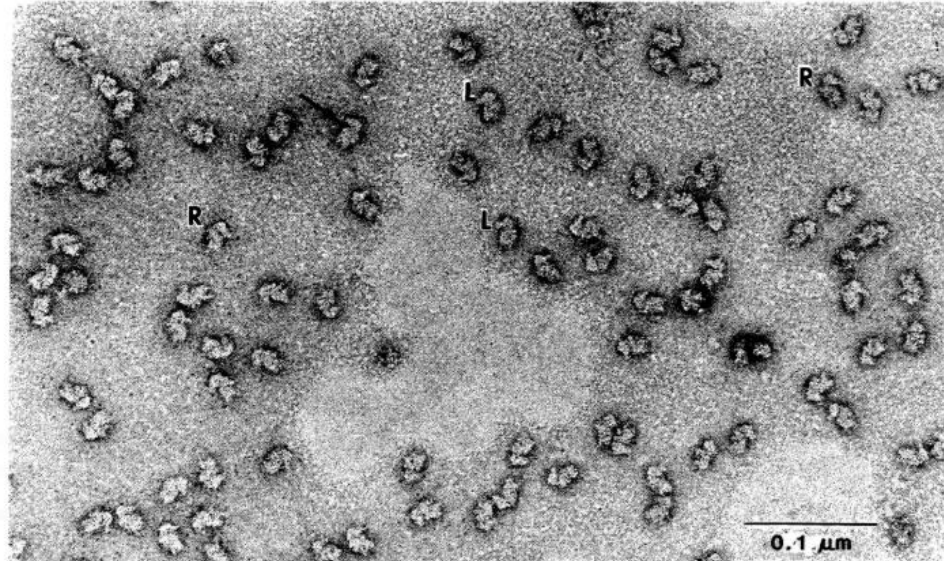
Jim Lake



In the beginning, there was the Lake model:
3D reconstruction by eye,
inferred from EM images

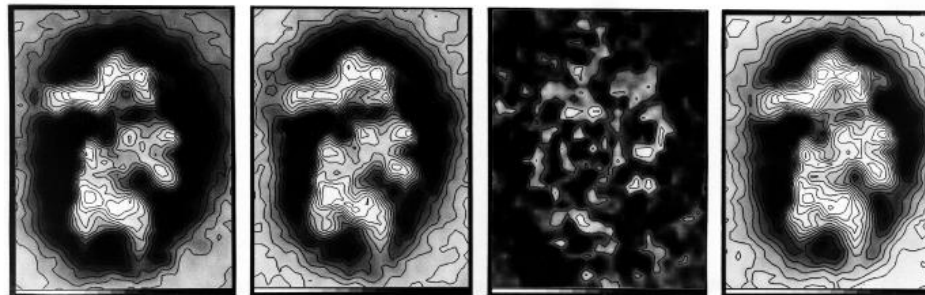
1970s

Alignment and averaging of single-particle images



Proof of concept

40S subunits of
HeLa (human)
Ribosomes



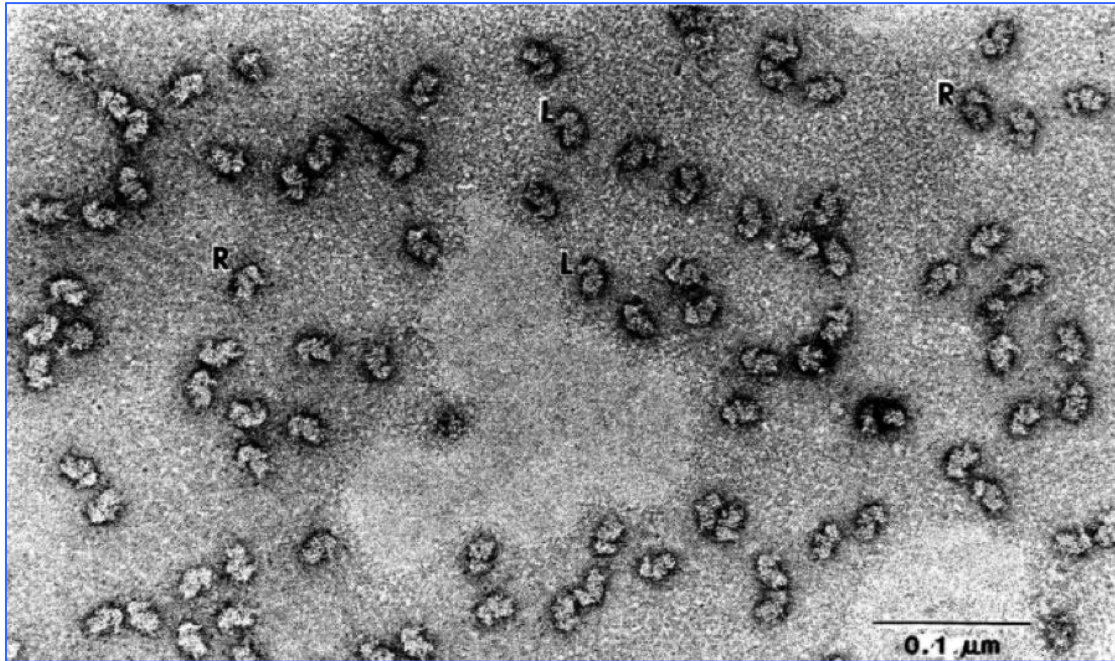
HALF-AVERAGES

S.D. MAP

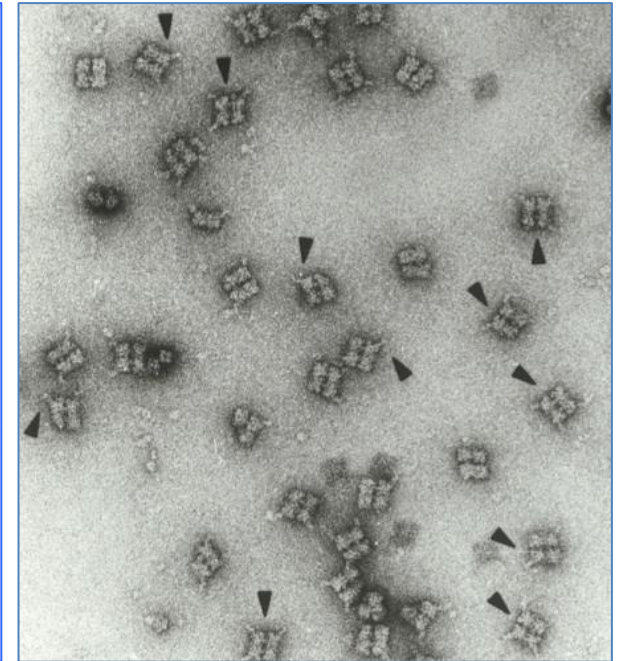
AVERAGE

Frank et al., Science 1981

Problem of heterogeneity: molecules are in different orientations and conformations



Frank et al., Science 1981

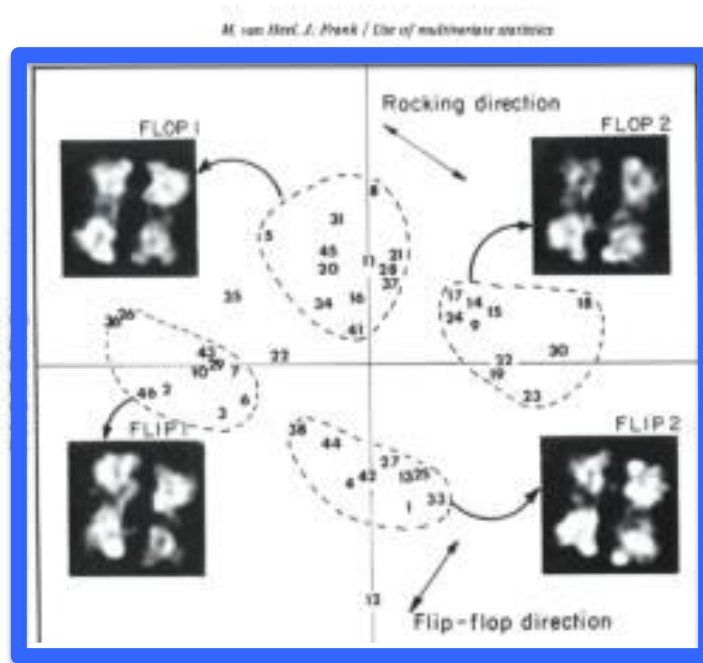


N. Boisset, thesis 1987

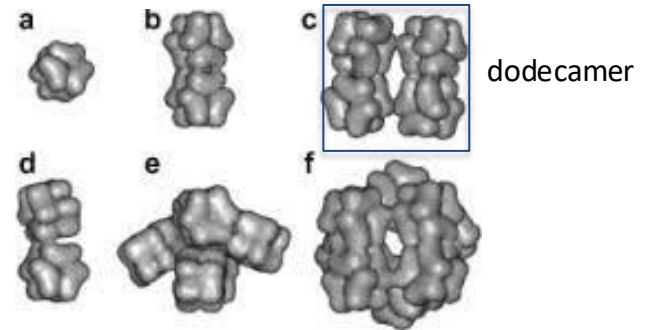
L and R views (flip and flop) of HeLa ribosomes

flip and flop views of hemocyanin

Multivariate analysis of aligned molecule images



FLIP/FLOP and Rocking positions



Hemocyanins of Arthropods are oligomers of a basic unit

Van Heel and Frank, Ultramicroscopy 1981

How to Find the Angles of Projection

Via bootstrap:

Random-conical tilt reconstruction

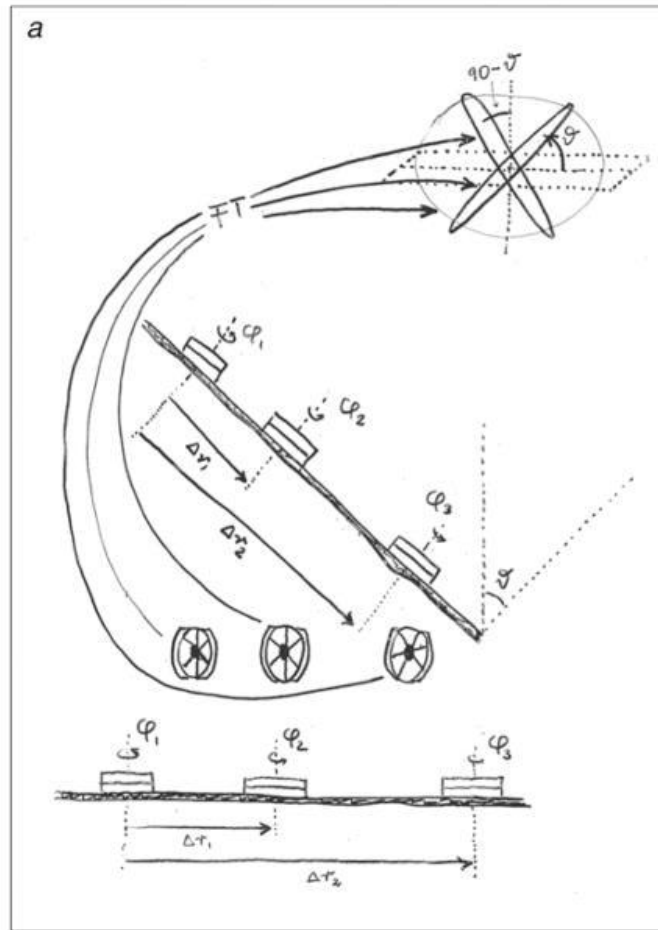
1979



1986/87

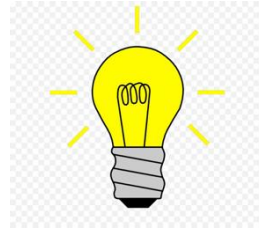


Random-Conical Tilt Reconstruction (Principle)



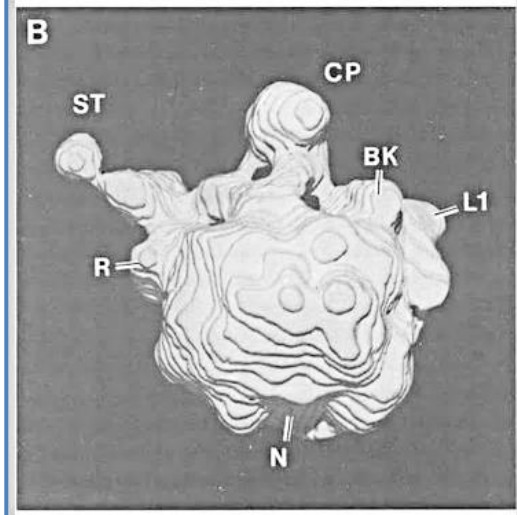
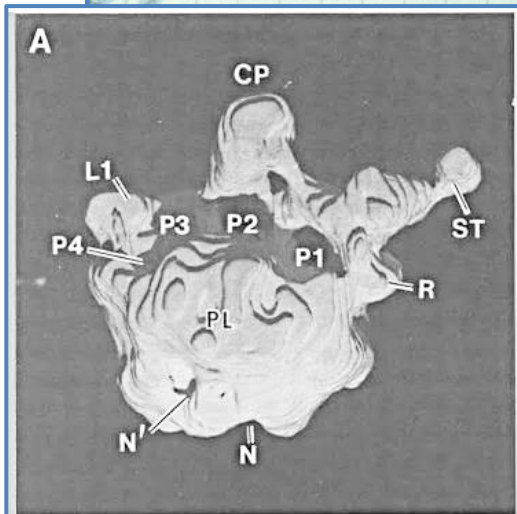
J. Frank, overhead 1979

Random-Conical Tilt Reconstruction (Principle – Fancy Version)



J. Frank, American Scientist 1998

First single-particle 3D reconstruction 1987



Michael Radermacher

The 50S ribosomal subunit
as a contour stack in 3D



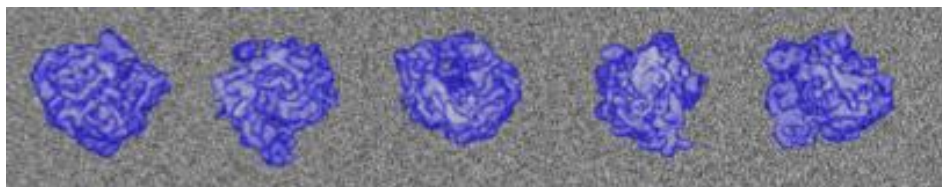
First 3D Reconstruction using Single Particle Reconstruction
Nobel Museum, Stockholm



Dario Fo

Dario Fo

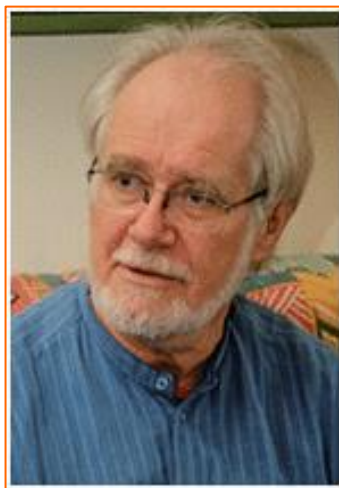
Frozen-hydrated specimens / Plunge-freezing / Vitreous ice / Cryo-EM



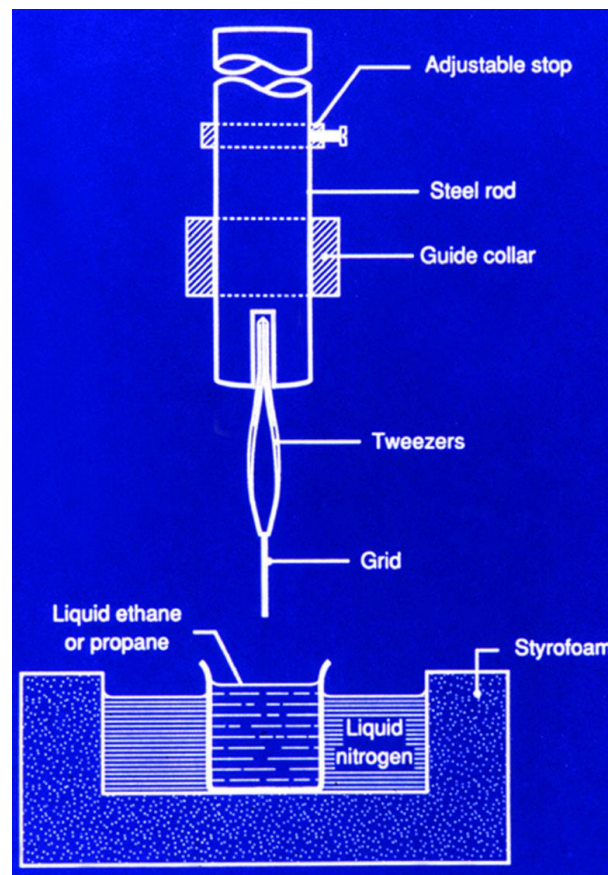
Molecules embedded in vitreous ice



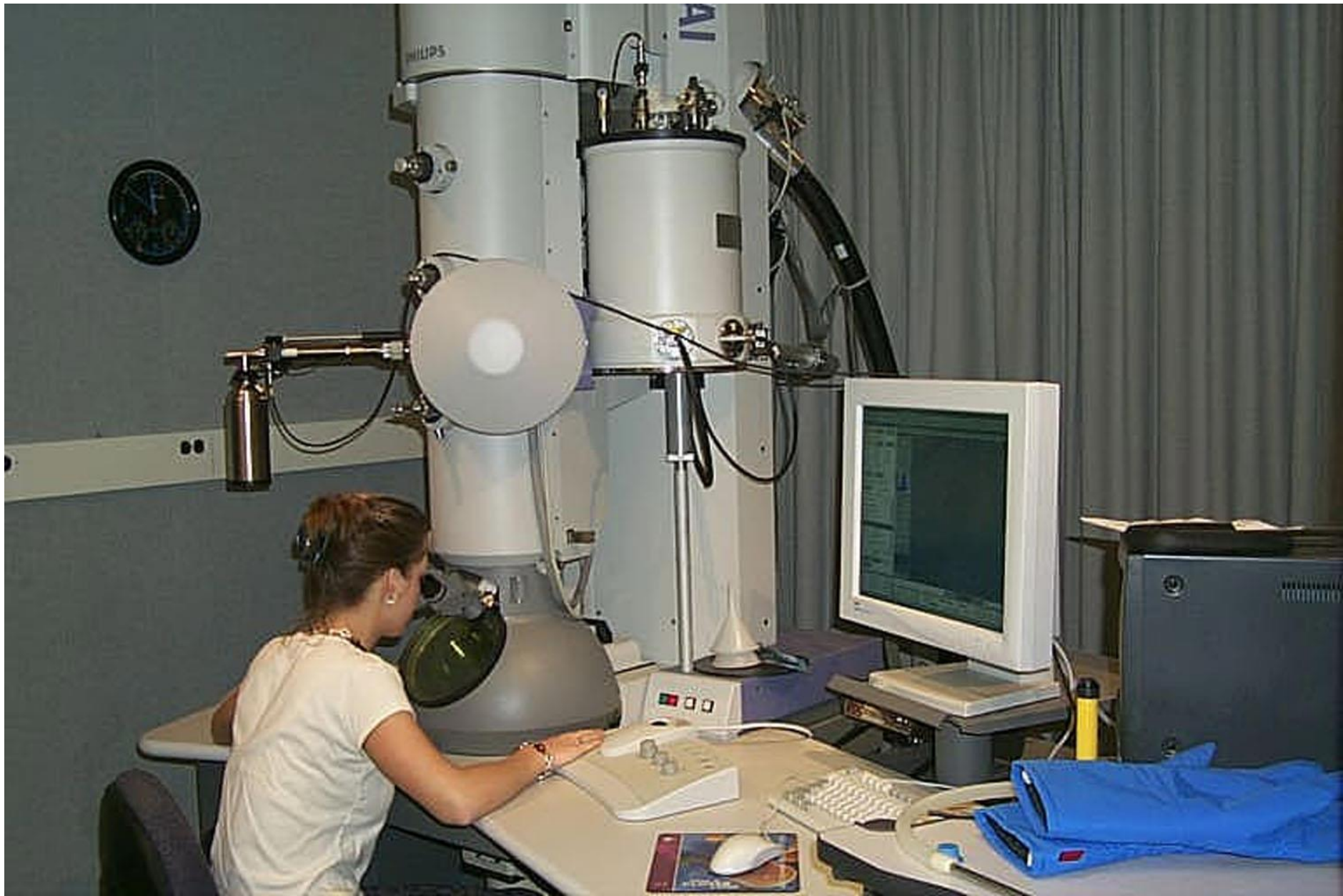
Robert Glaeser
1976



Jacques Dubochet
1981



Plunge-freezer

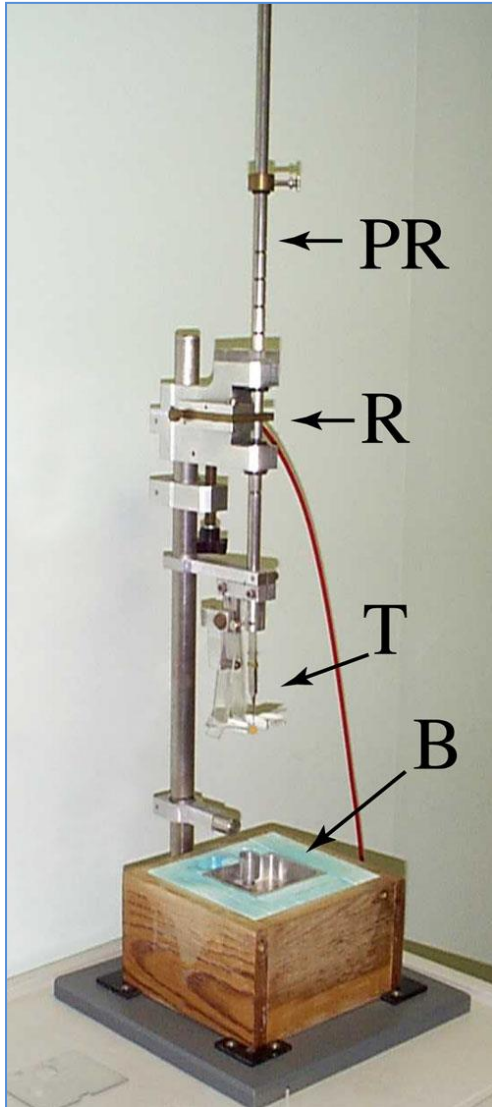


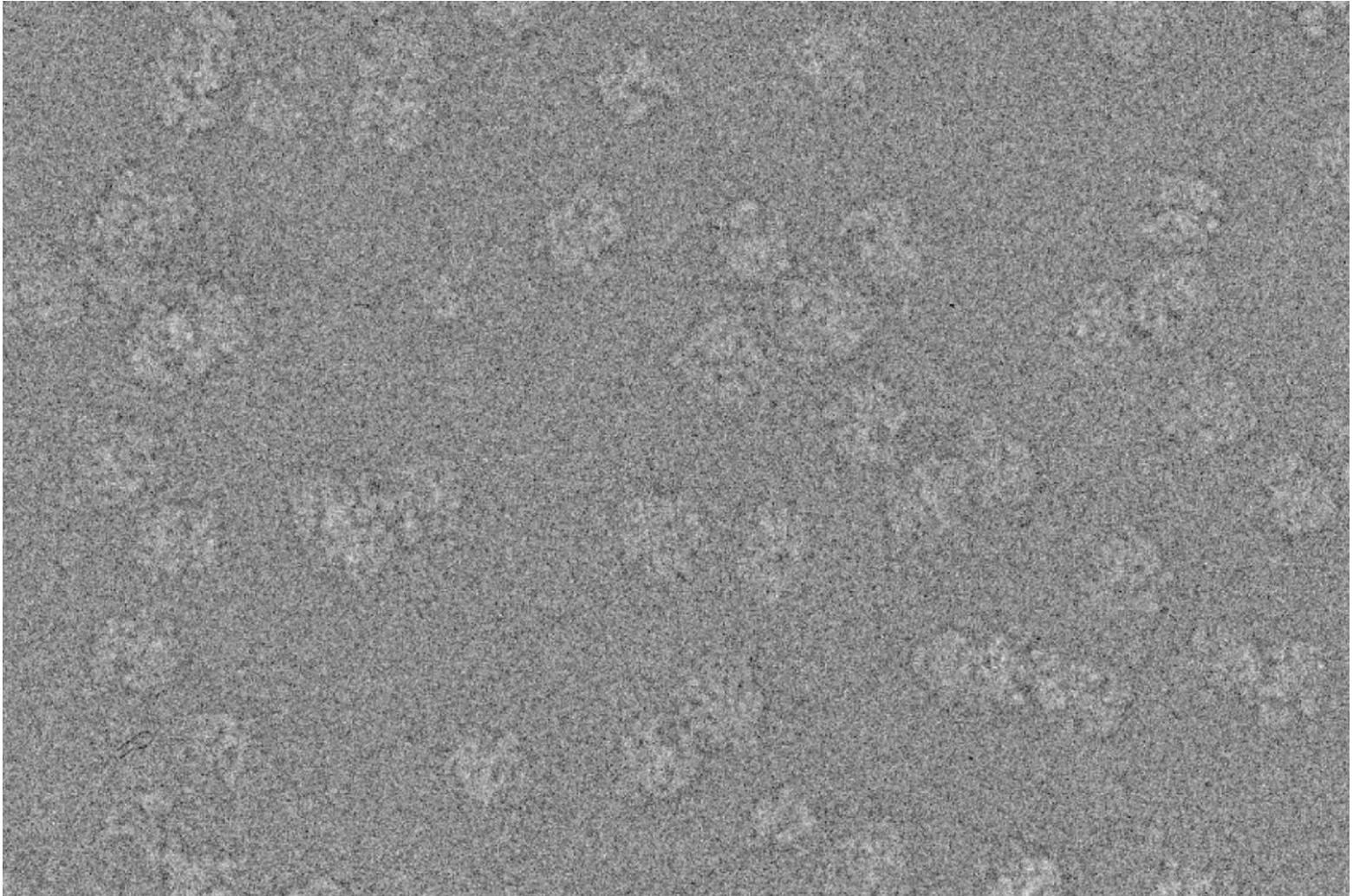
F30 Polara (FEI)

Plunge-freezers

----- manual -----

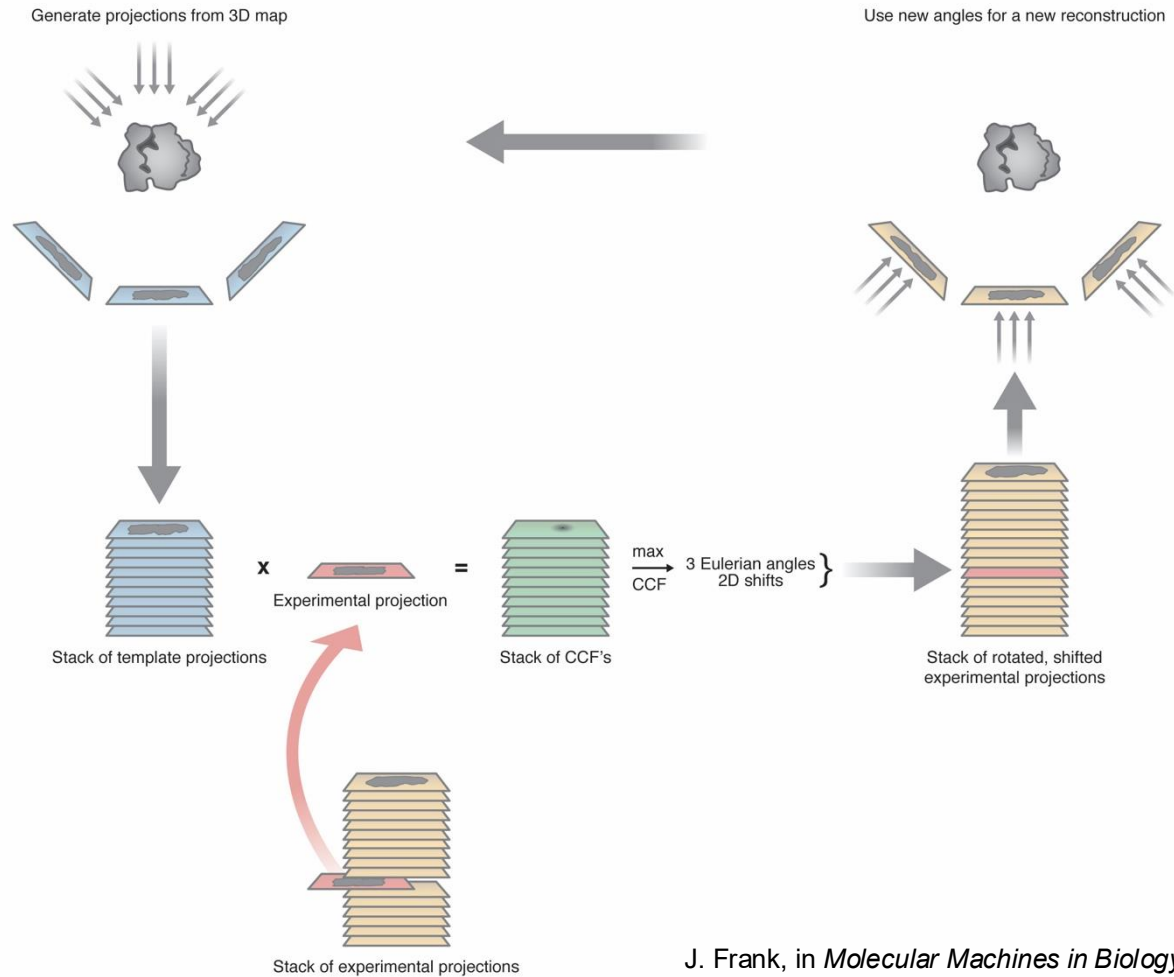
----- automated, climatized -----





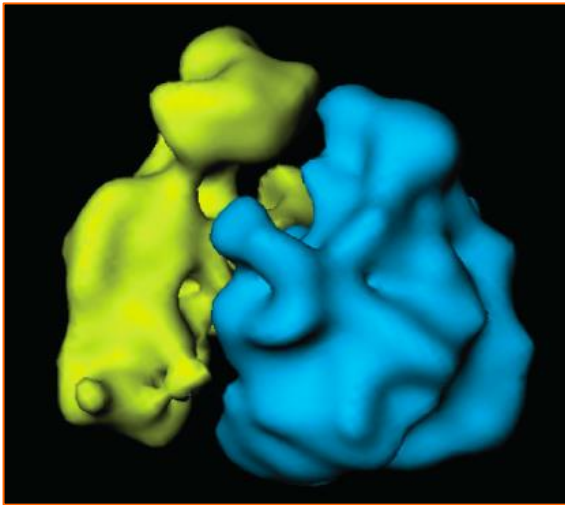
ribosomes, recorded on film: poor quality of recording

Iterative angular refinement



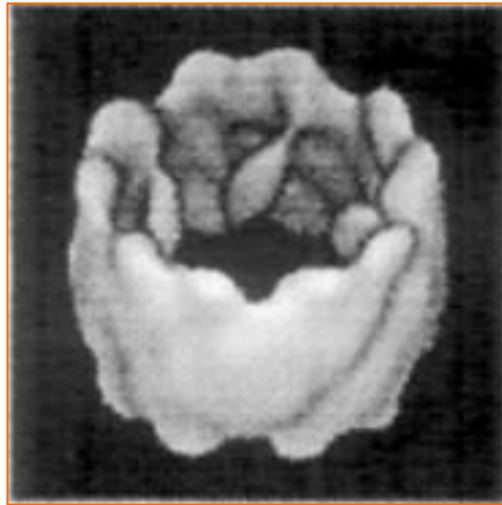
J. Frank, in *Molecular Machines in Biology* 2011

E. coli ribosome



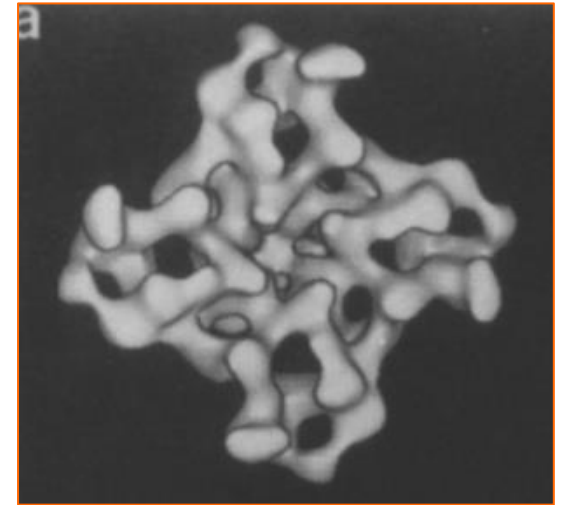
Frank et al., Nature 1995

Octopus hemocyanin

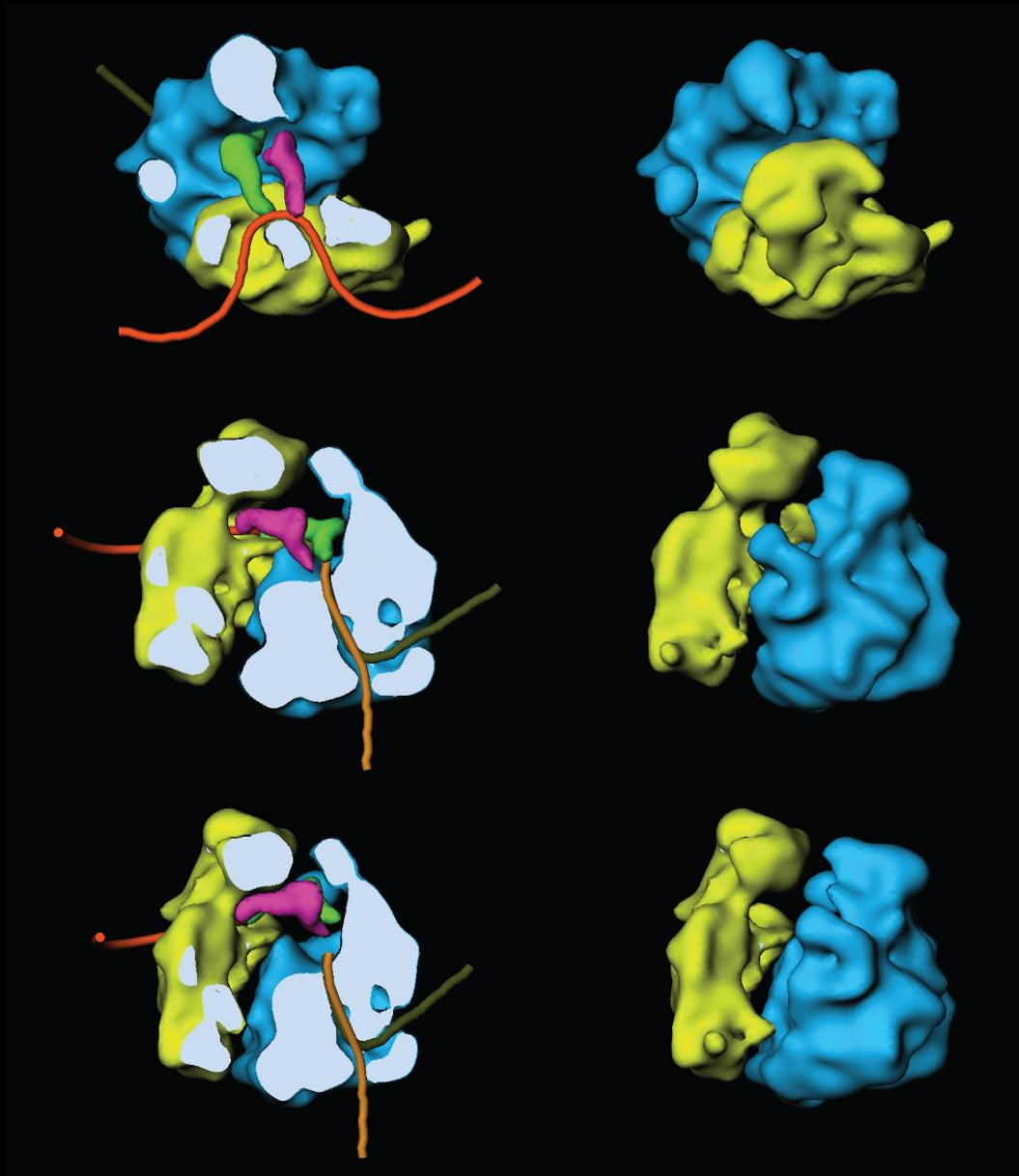


Lambert et al., 1994

Calcium Release Channel



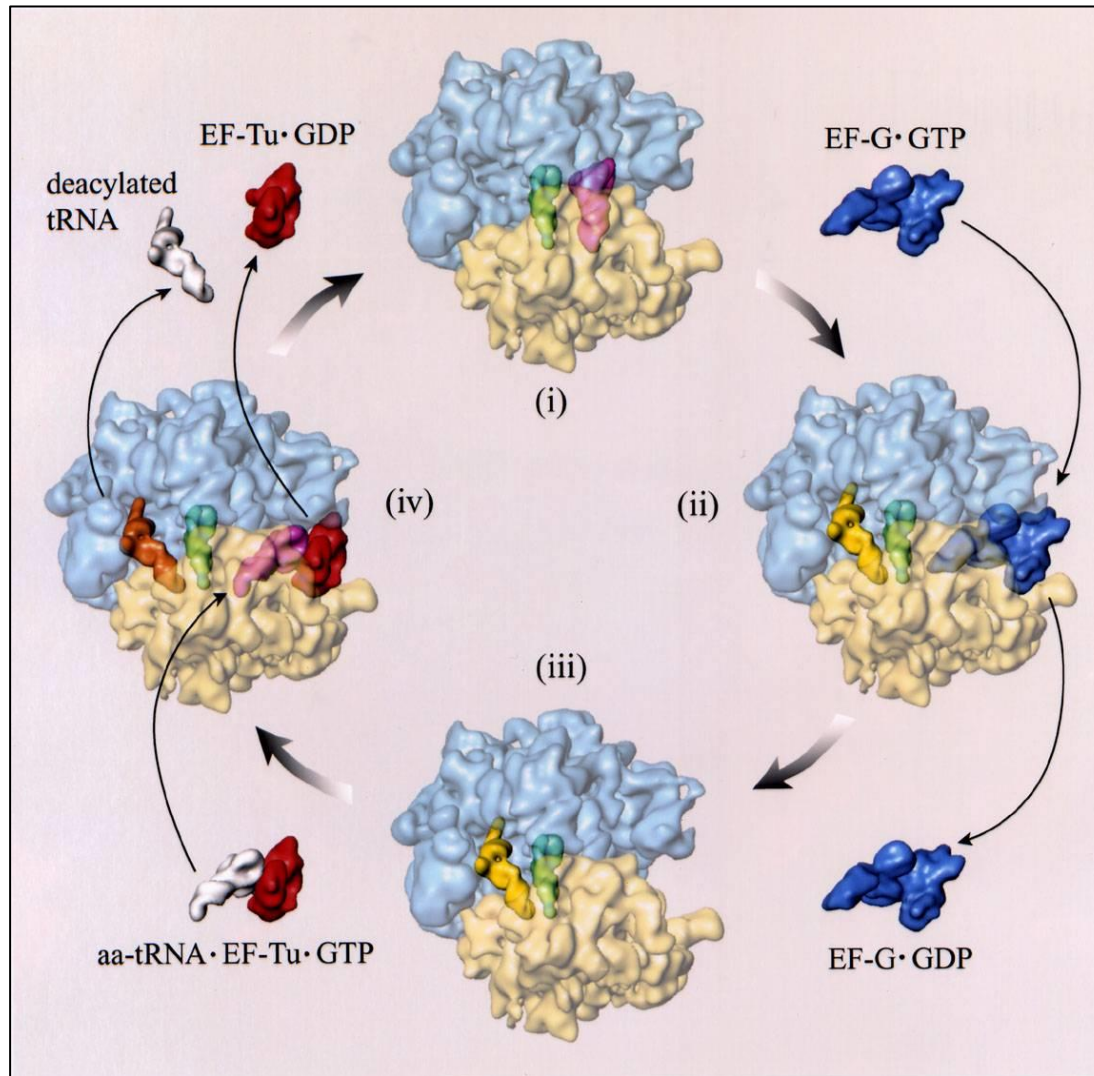
Radermacher et al., 1994



E. coli ribosome 1995

Elongation Cycle (for adding each amino acid)

Decoding



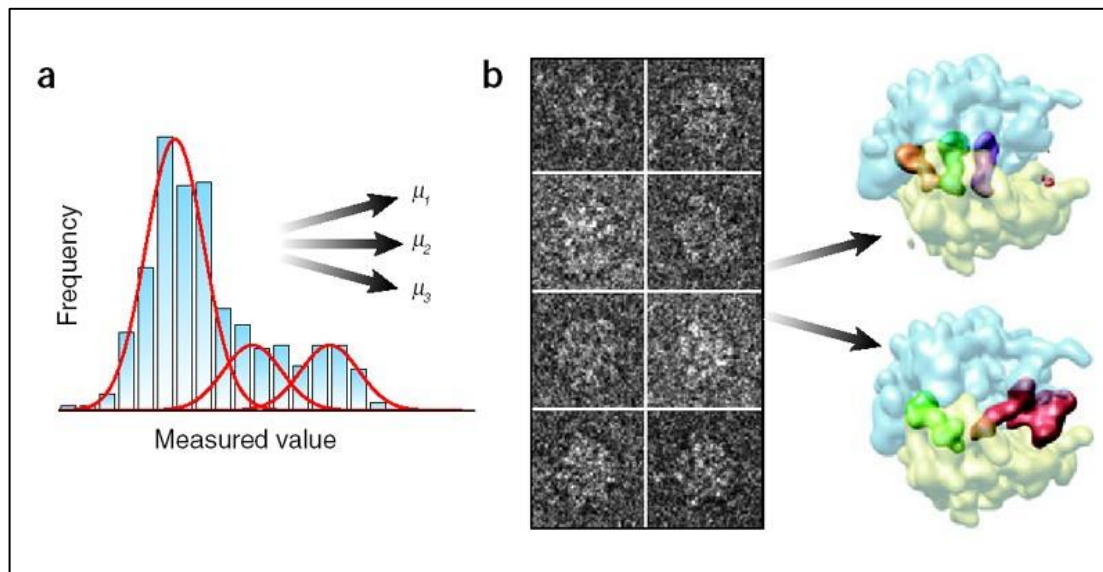
Translocation

Maximum likelihood method of classification

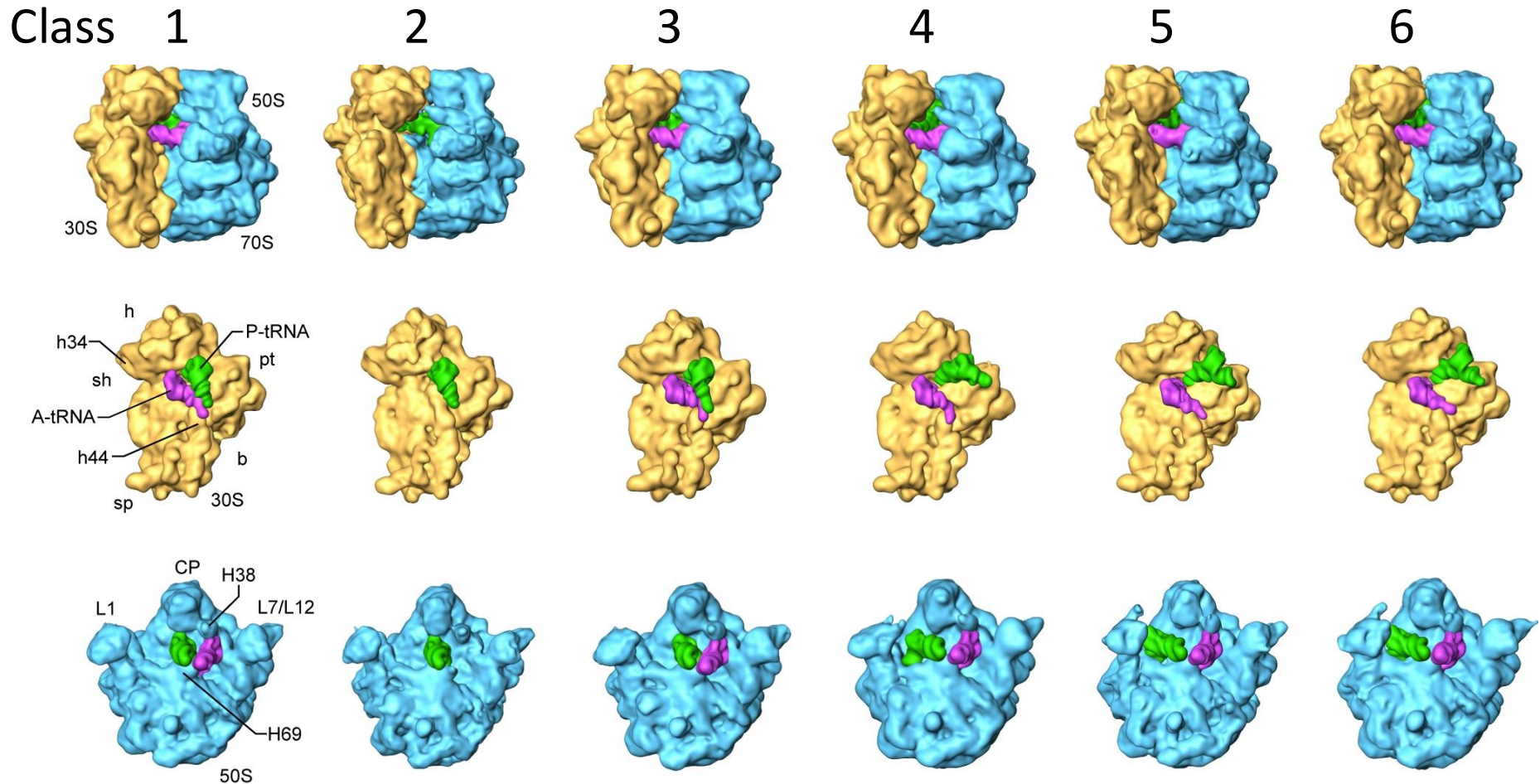
Several reconstructions from the same sample all at once!
"STORY IN A SAMPLE"

S.H.W. Scheres, H. Gao, M. Valle, G.T. Herman, P.P.B. Eggermont, J. Frank & J.M. Carazo (2007). "Disentangling conformational states of macromolecules in 3D-EM through likelihood optimization." *Nat. Methods*, 4, 27-29.

S.H.W. Scheres (2012). "A Bayesian View on Cryo-EM Structure." *J. Mol. Biol.* 415, 406-418.

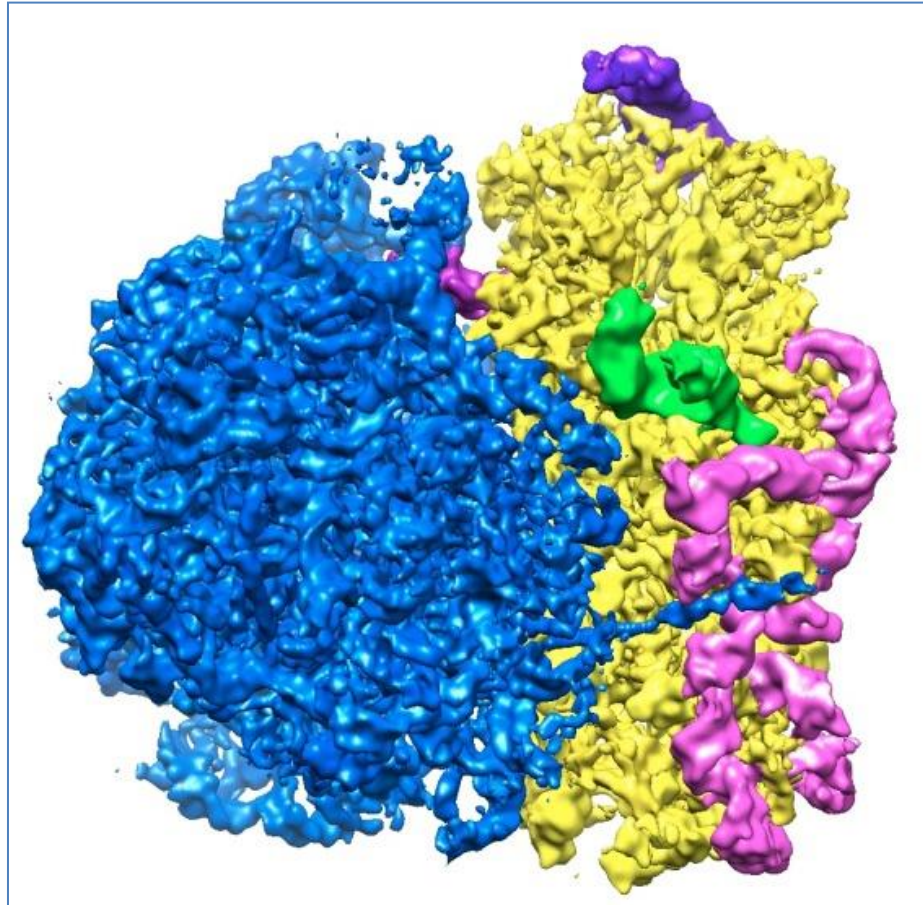


“STORY IN A SAMPLE” -- intermediate states in the ratchet-like motion and hybrid tRNA positions in the absence of EF-G



Agirrezabala et al., PNAS 2012

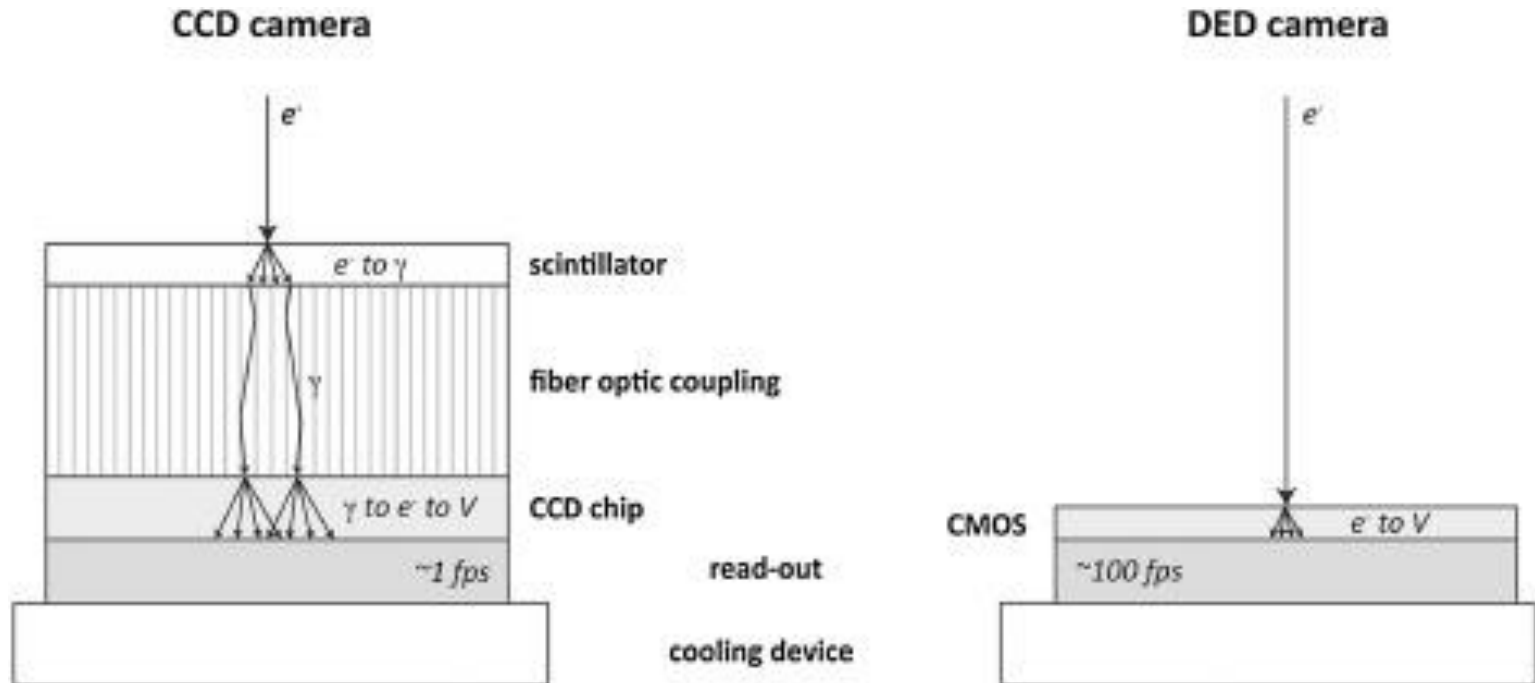
Resolution of single-particle cryo-EM was limited by the inferior quality of the recording medium



Hashem et al., Nature 2013

Best resolution from recording on film: 5.5Å

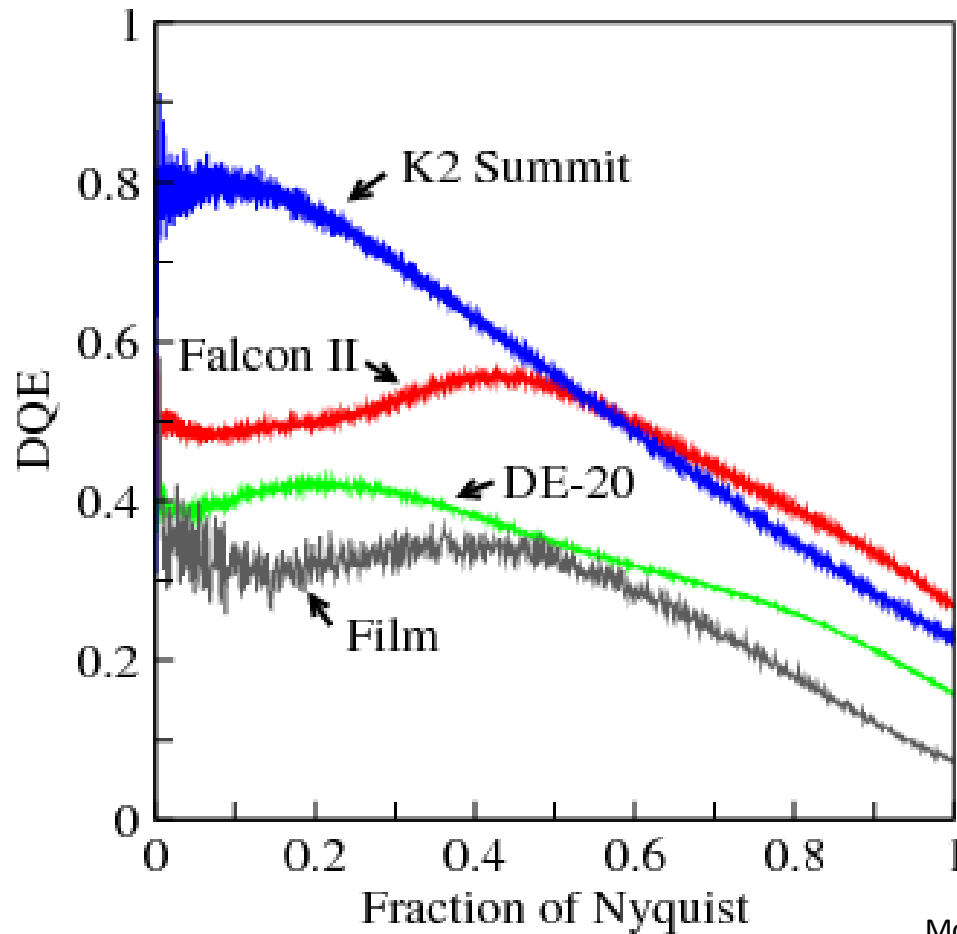
NEW ERA (SINCE 2012): DIRECT ELECTRON DETECTING CAMERAS

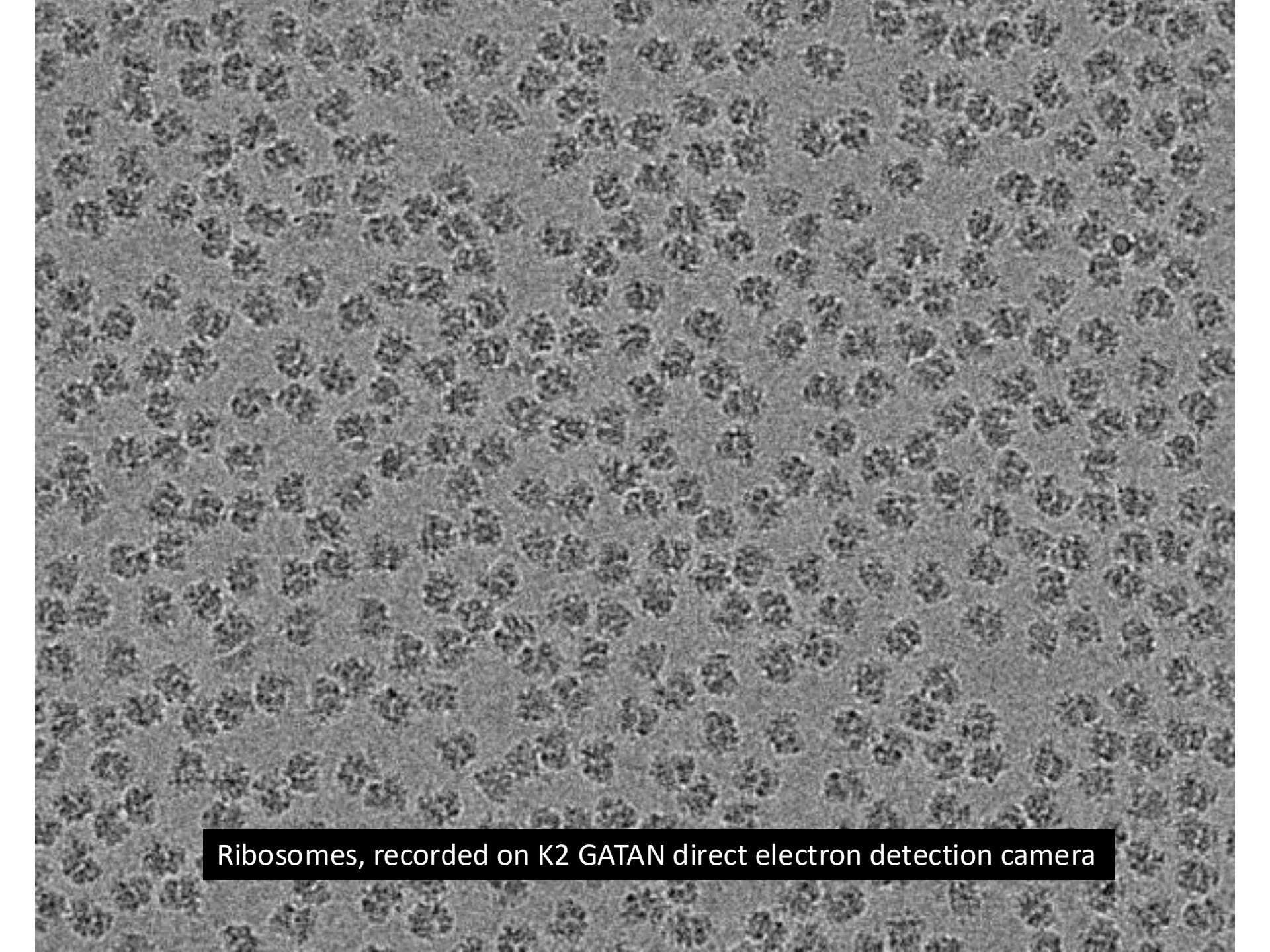


New era (since 2012): *New single-electron detecting cameras*

Detection Quantum Efficiency (DQE):

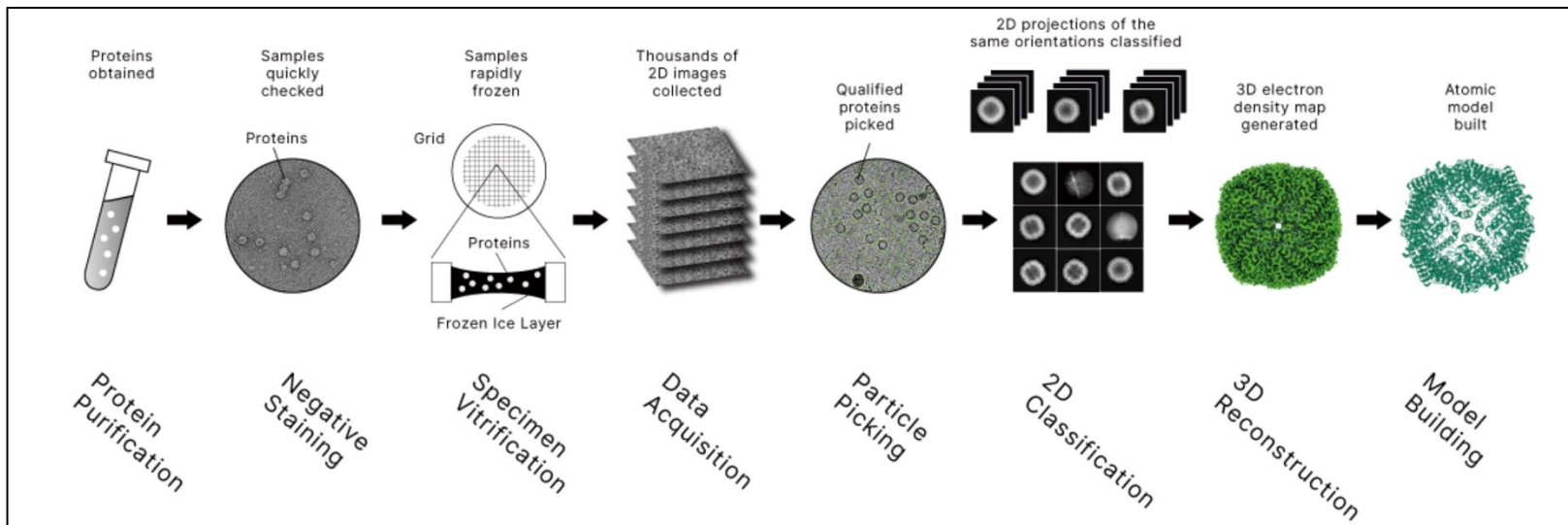
(how good is the recording device in capturing every single electron?)





Ribosomes, recorded on K2 GATAN direct electron detection camera

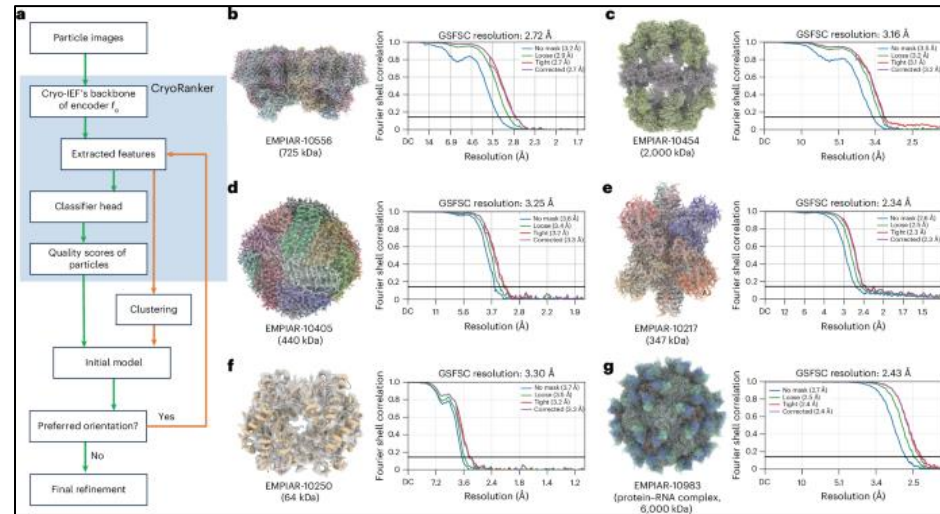
WORKFLOW FROM SAMPLE TO ATOMIC STRUCTURE



<https://shuimubio.com/services/cryo-em-spa>

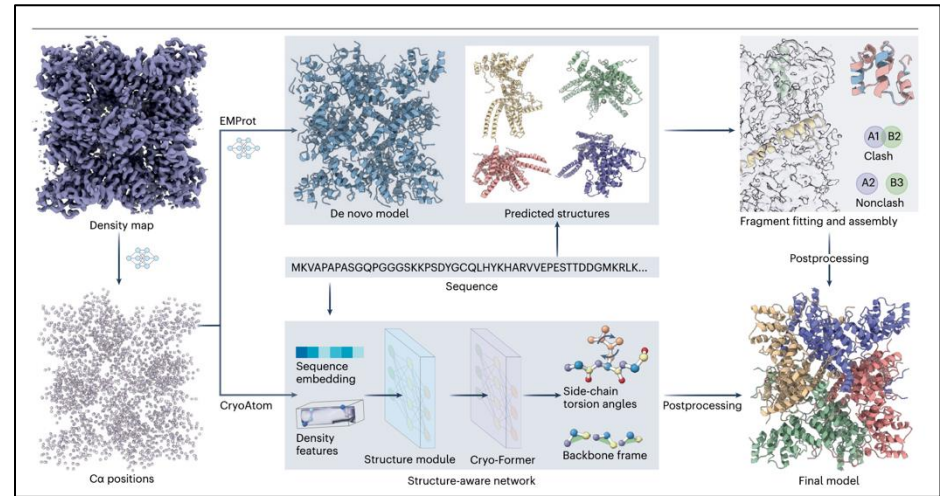
NEW: Atomic model building from single-particle cryo-EM assisted by machine learning

CryoWizard: Yang Yan ... Huaizong Shen. A comprehensive foundation model for cryo-EM image processing. *Nat Meth* (2026)



Cryo-Atom: Baoquan Su ... Jianyi Yang. CryoAtom improves model building for cryo-EM. *Nat Struct Mol Biol* (2025)

EMProt: Tao Li ... Sheng-You Huang. EMProt improves structure determination from cryo-EM maps. *Nat Struct Mol Biol* (2025)



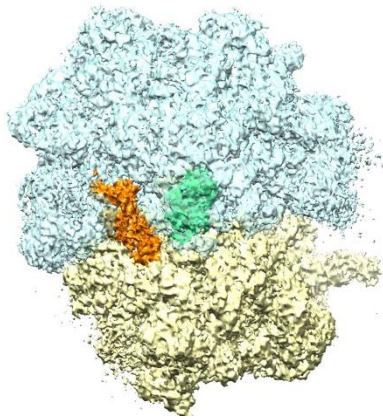
Elongation Factor G mutant H94A bound to the ribosome

nr 70S--P-E

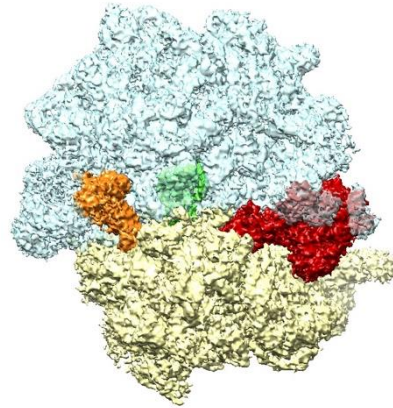
nr 70S--EF-G--P-E

r 70S--EF-G--P/E

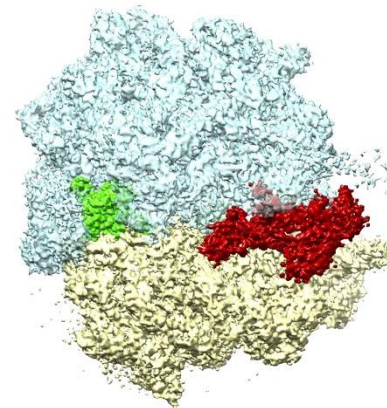
r 70S--P/E



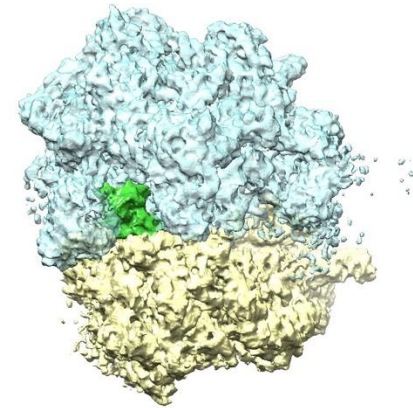
50,000



90,000



35,000

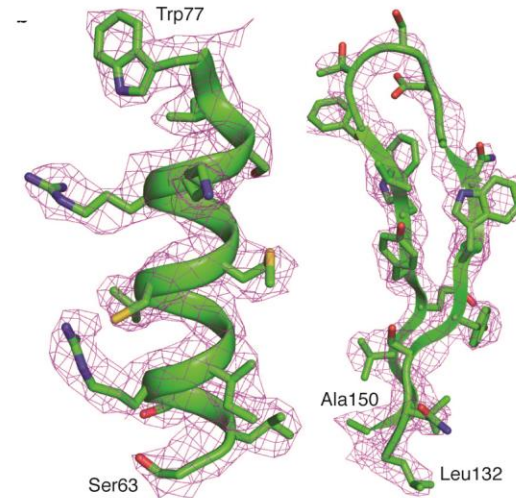
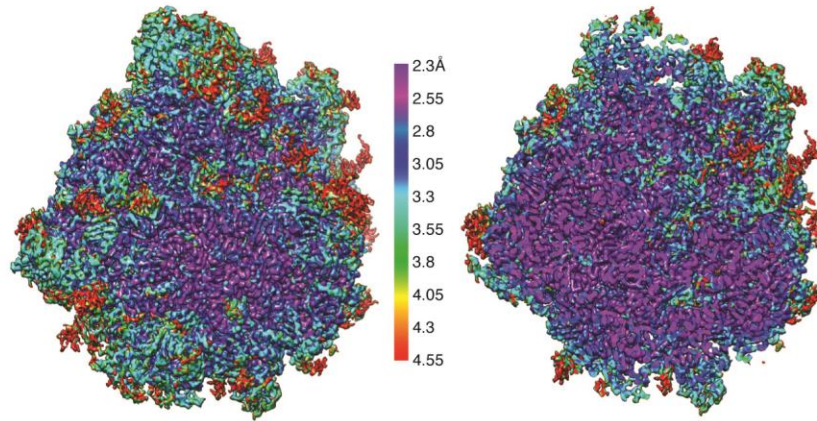


15,000

Example for maximum likelihood 3D classification
Multiple states in the same sample

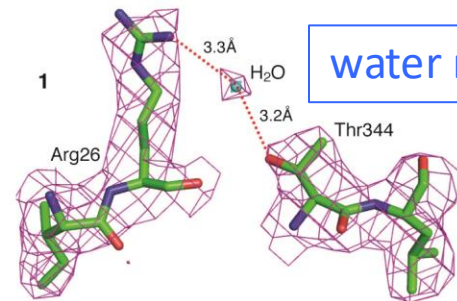
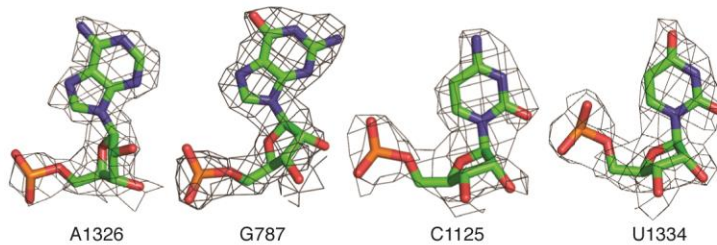
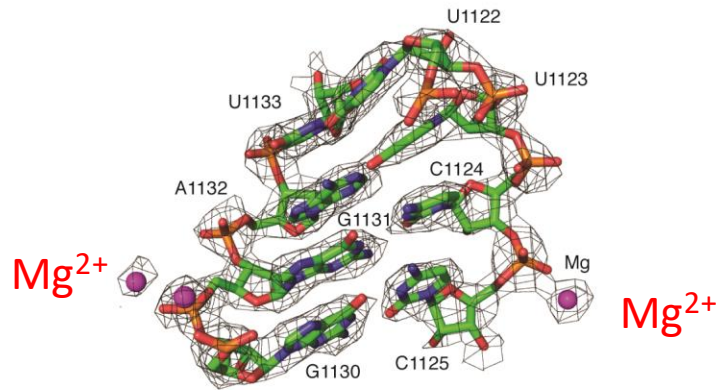
T. cruzi ribosome large subunit at 2.5 Å

Liu et al., PNAS 2016

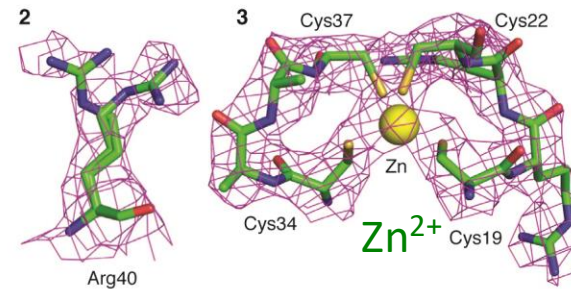


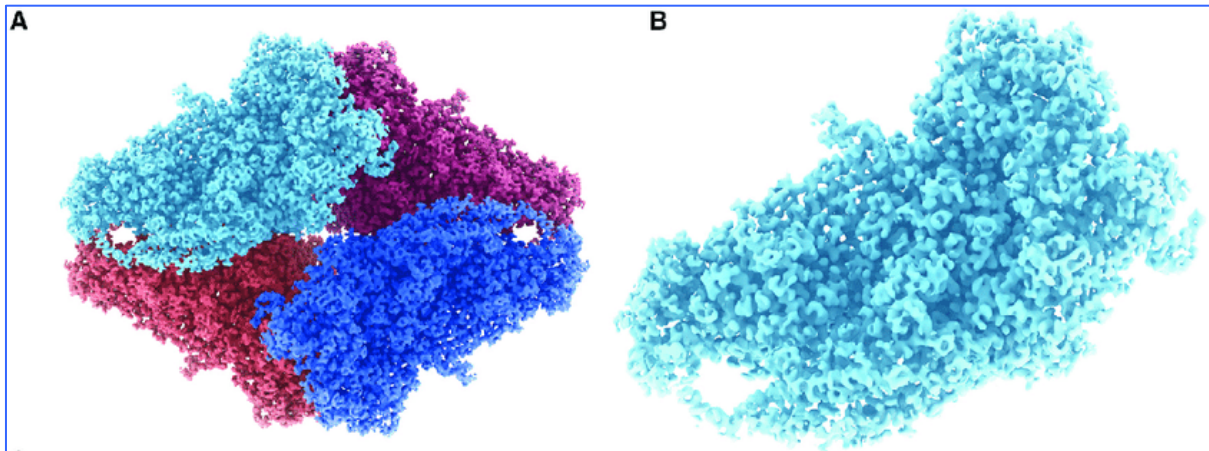
α -helix

2 strands of β -sheet



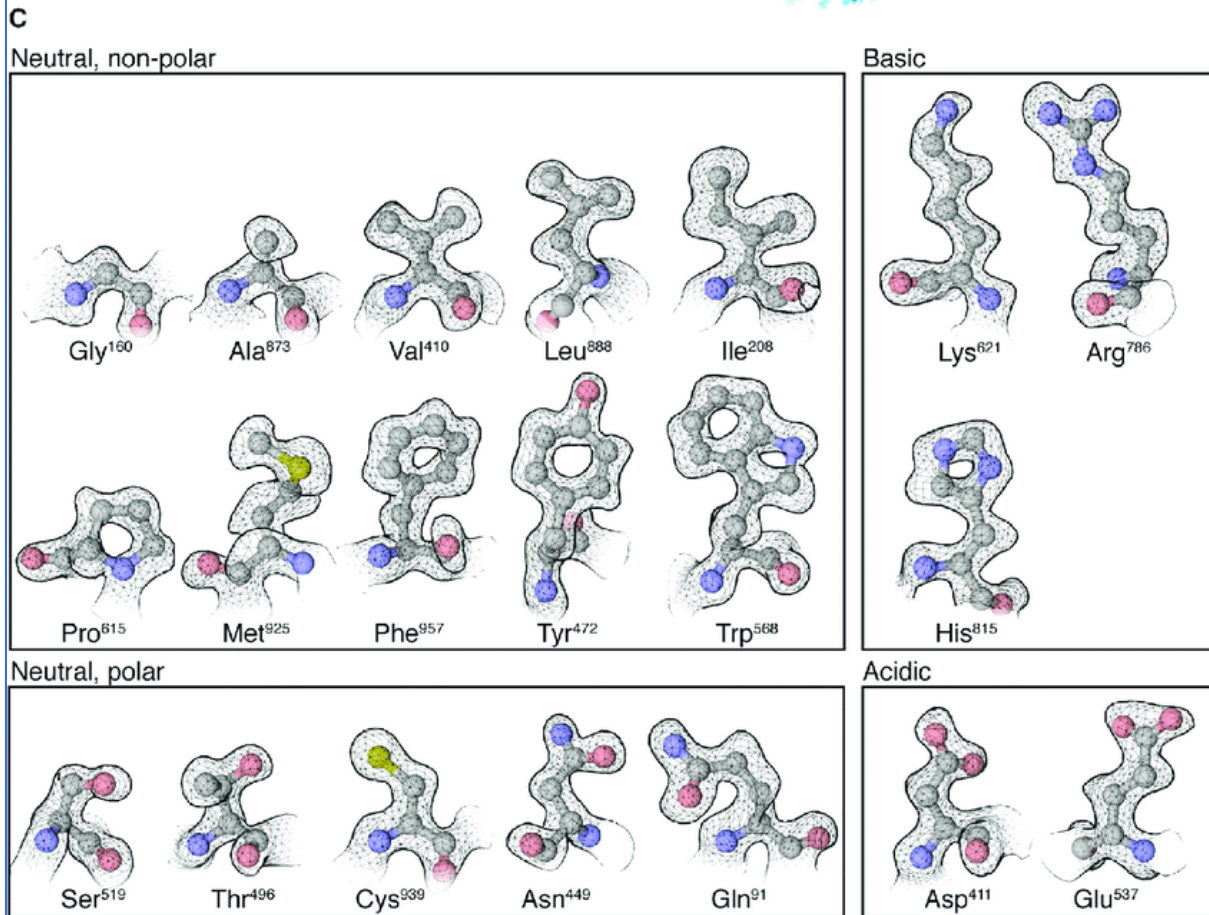
water molecule!





Bartesaghi et al.
STRUCTURE 2018

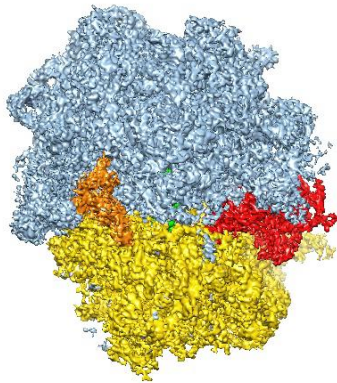
Beta-Galactosidase
At 2.2 Å resolution



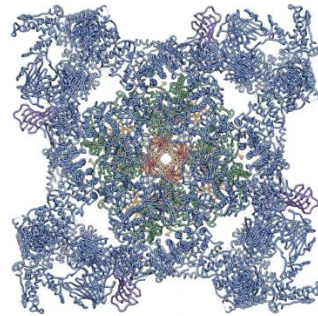
“Signatures” of
amino acids in the
Coulomb density
distribution

What has been achieved by single-particle cryo-EM to date?

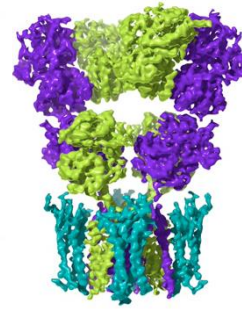
-- thousands of structures from labs worldwide. Below a few examples from Columbia and specifically my lab:



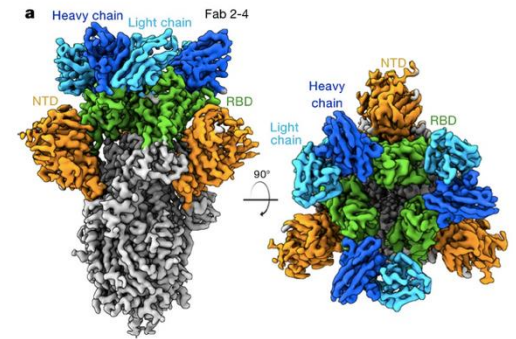
T. cruzi ribosome
Liu et al.,
PNAS 2016



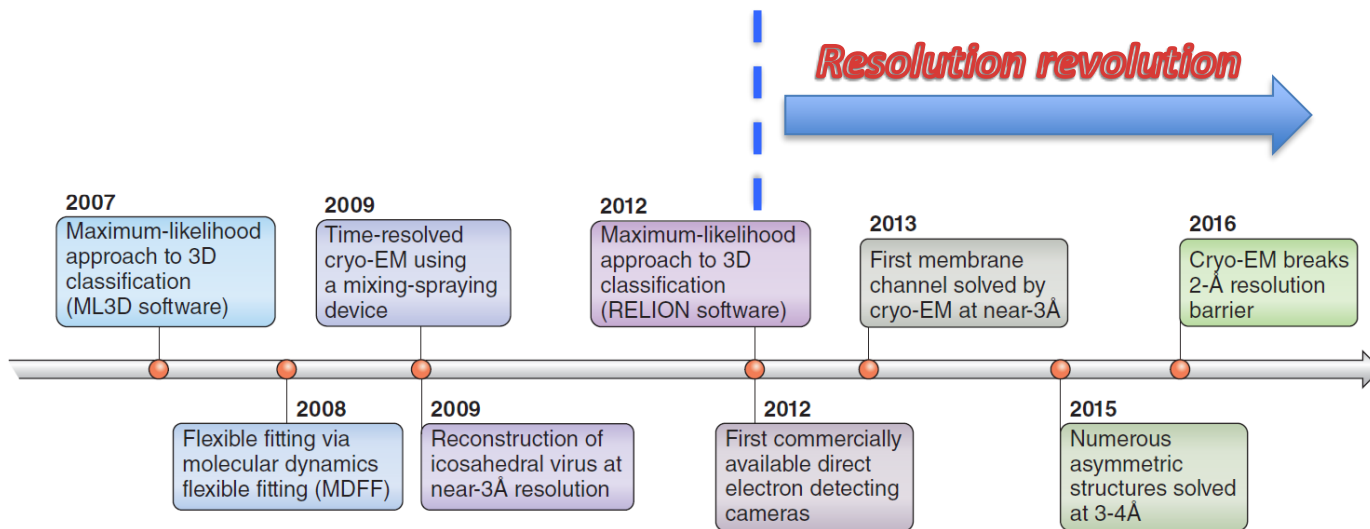
Calcium release channel
Des Georges et al.,
Cell 2017



AMPA receptor
Twomey et al.,
Nature 2017



SARS-Cov-2 spike protein
epitope mapping. Liu et al.
Nature 2020



J. Frank, Nature Protocols 2017

Just in Time: high-resolution single-particle cryo-EM and the new pandemics

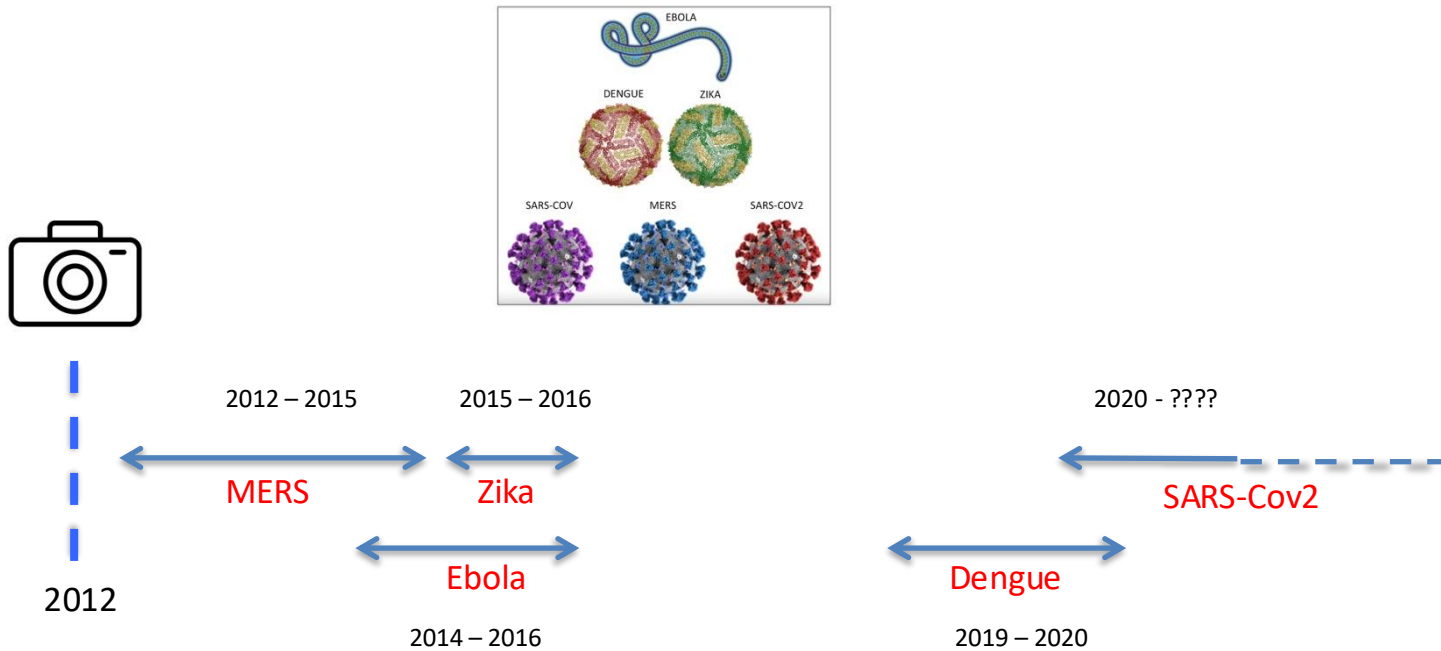
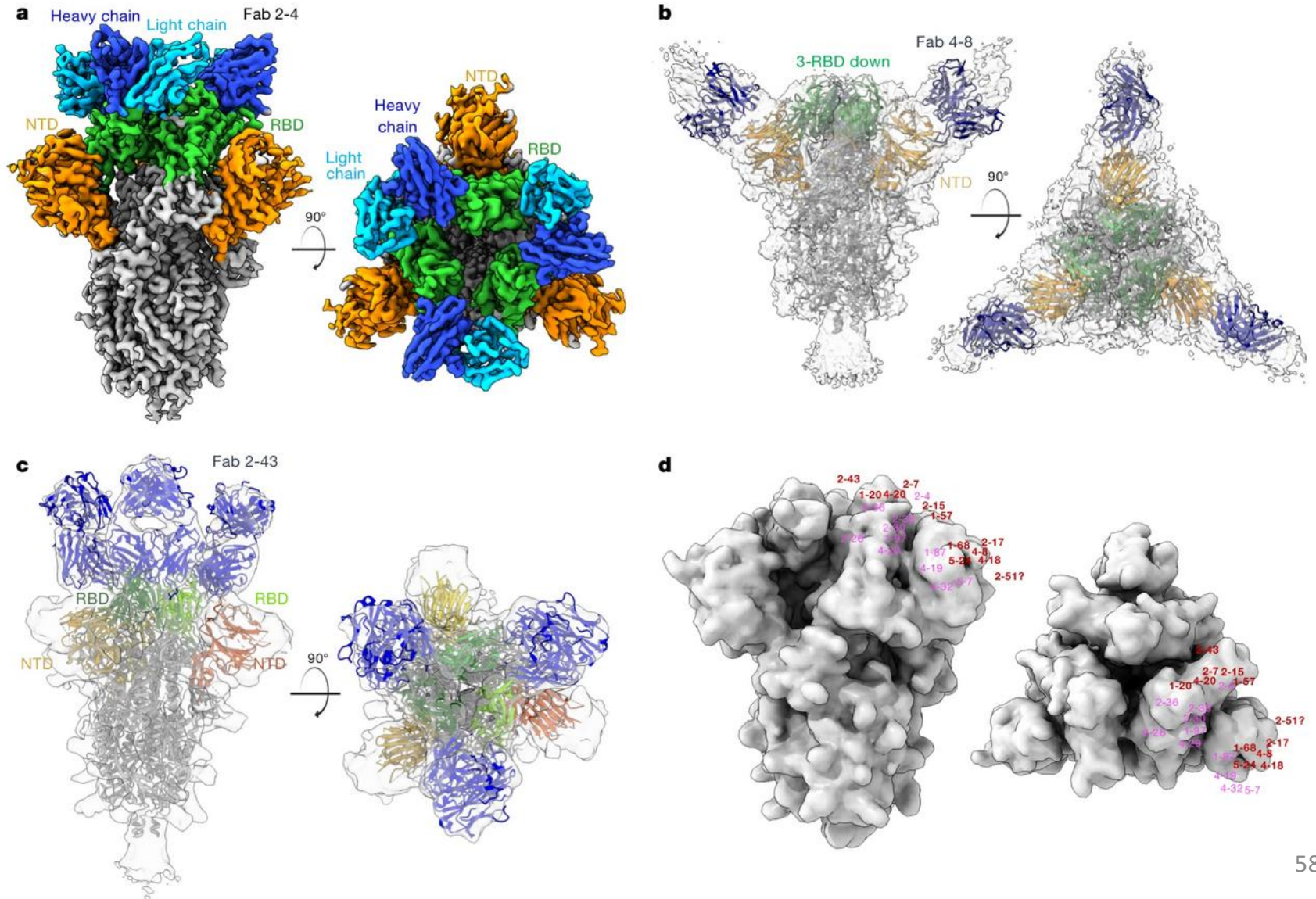
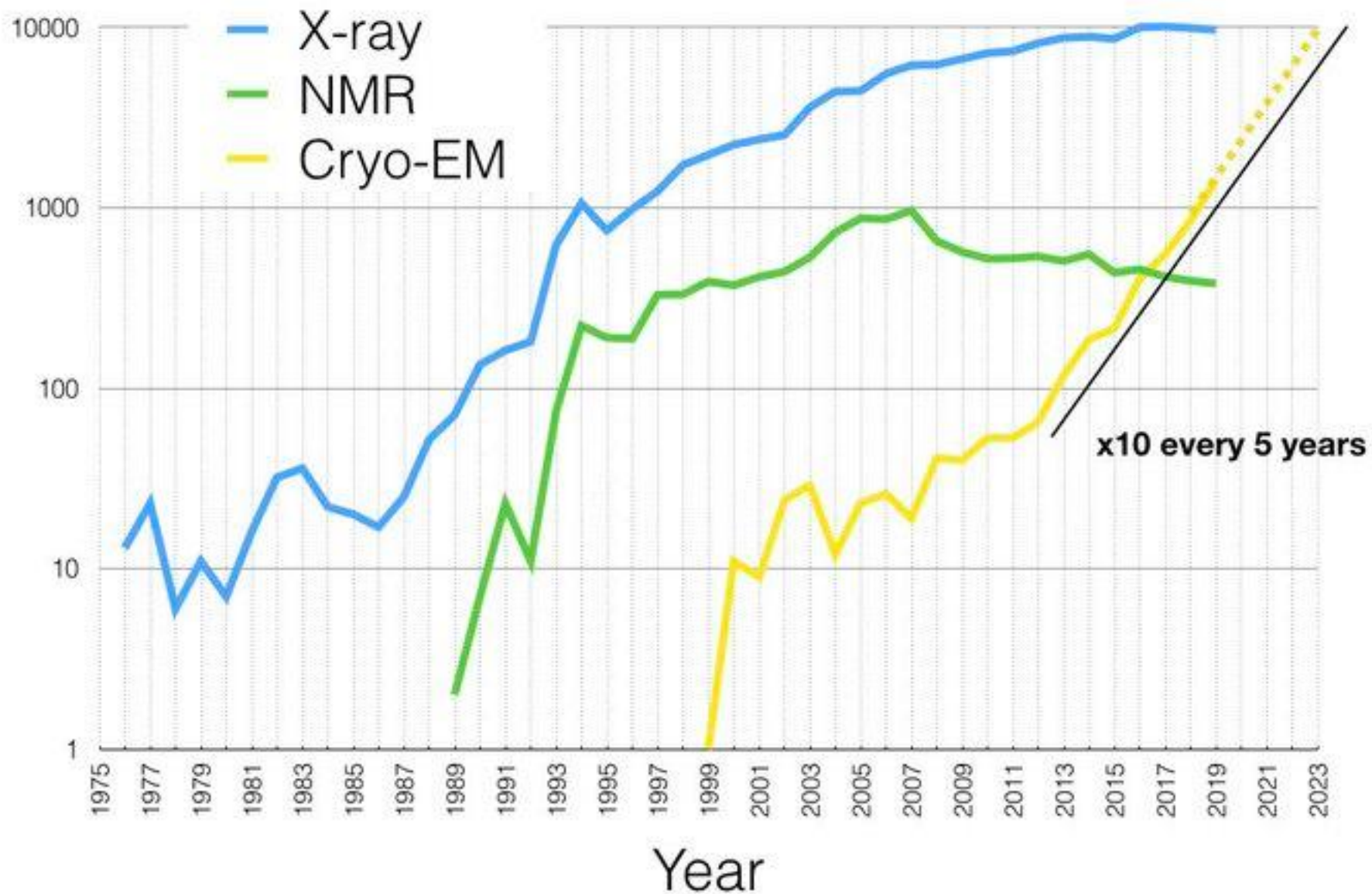


Fig. 4: Cryo-EM reconstructions of Fab-spike complexes and visualization of neutralizing epitopes on the spike surface.

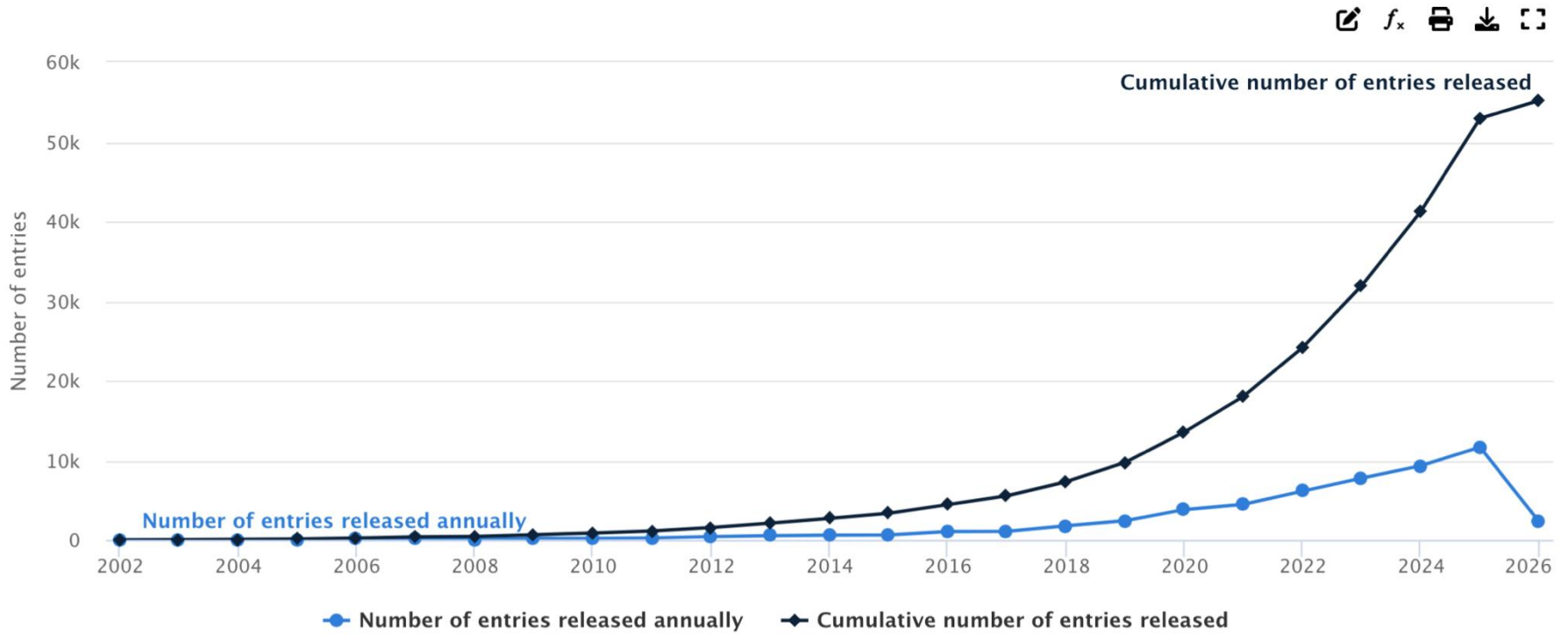
From: Potent neutralizing antibodies against multiple epitopes on SARS-CoV-2 spike



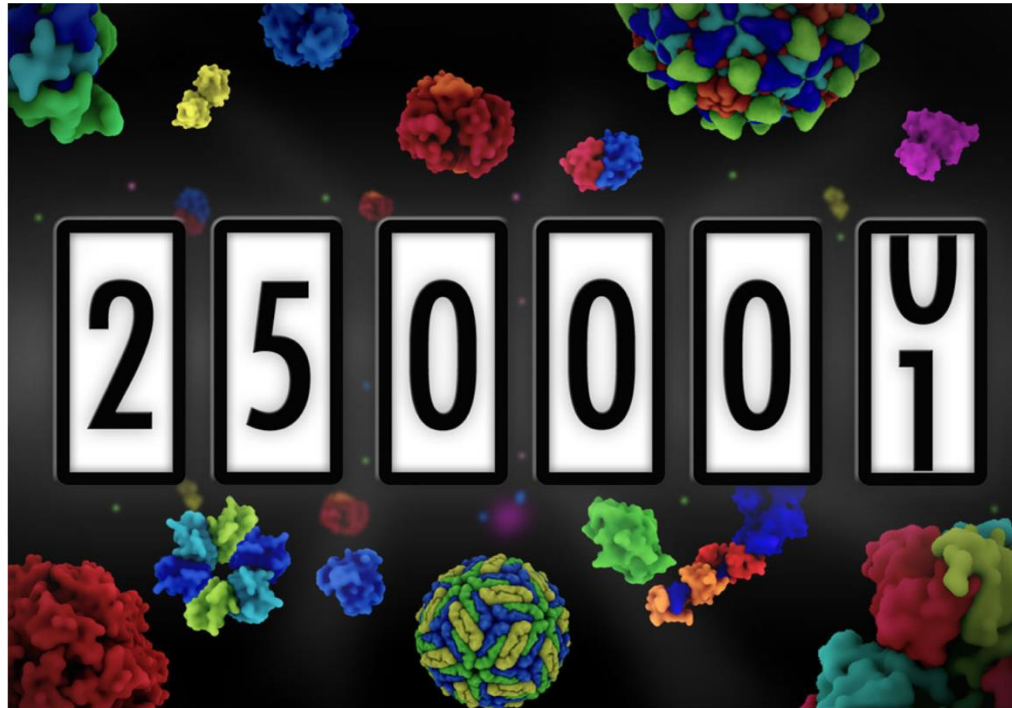
of released structures (PDB) / year



EMDB entries released per year and cumulatively

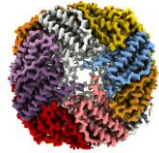


PDB Reaches a New Milestone



The PDB contains more than 250,000 entries

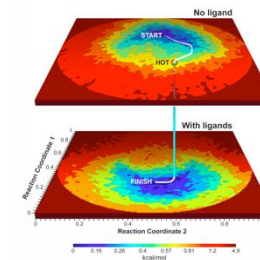
Future directions



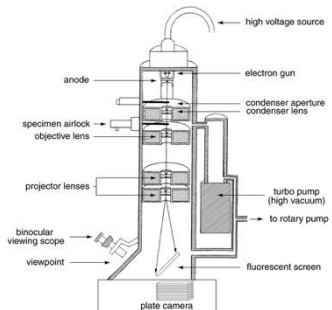
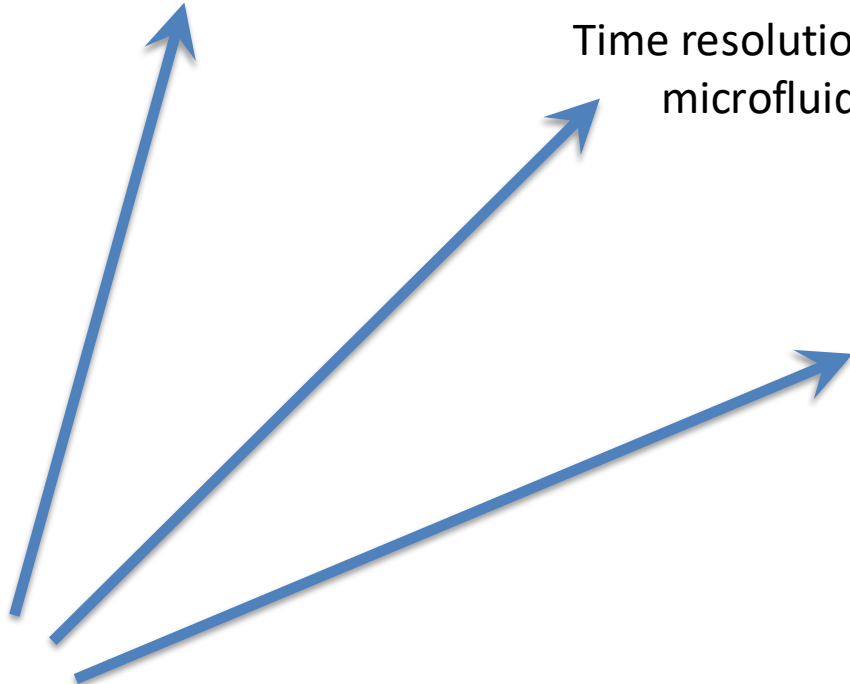
Higher spatial resolution



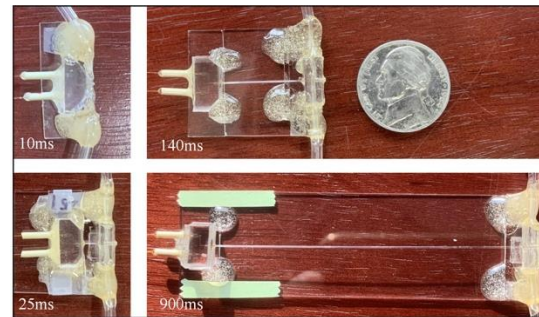
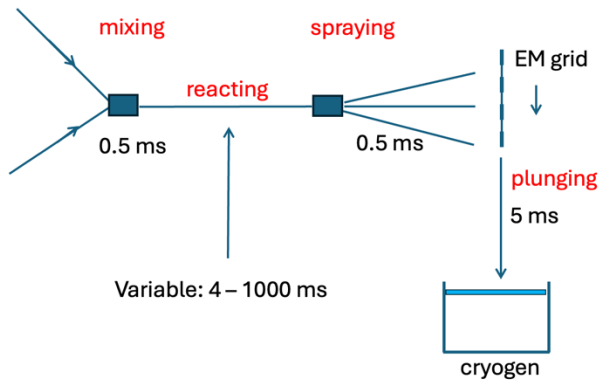
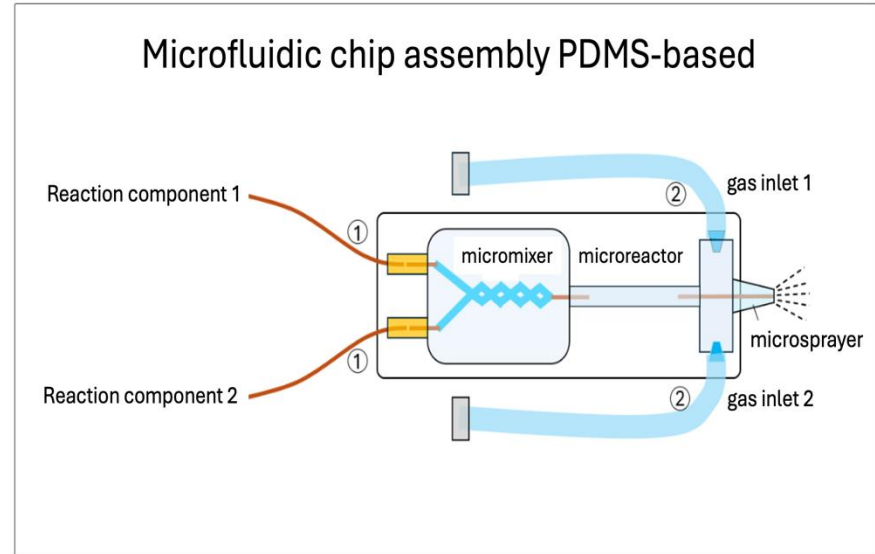
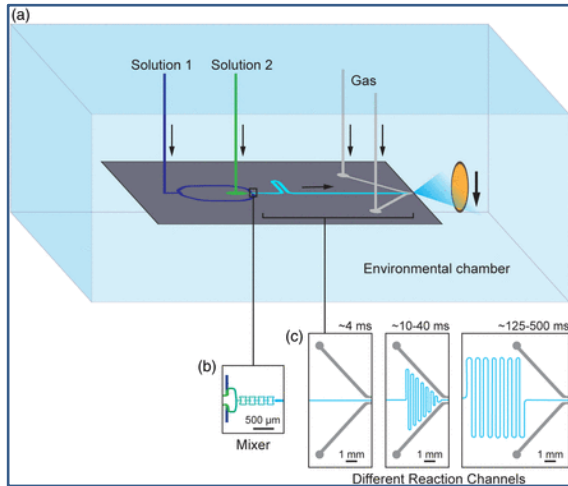
Time resolution
microfluidics



State resolution
machine learning
energy landscape

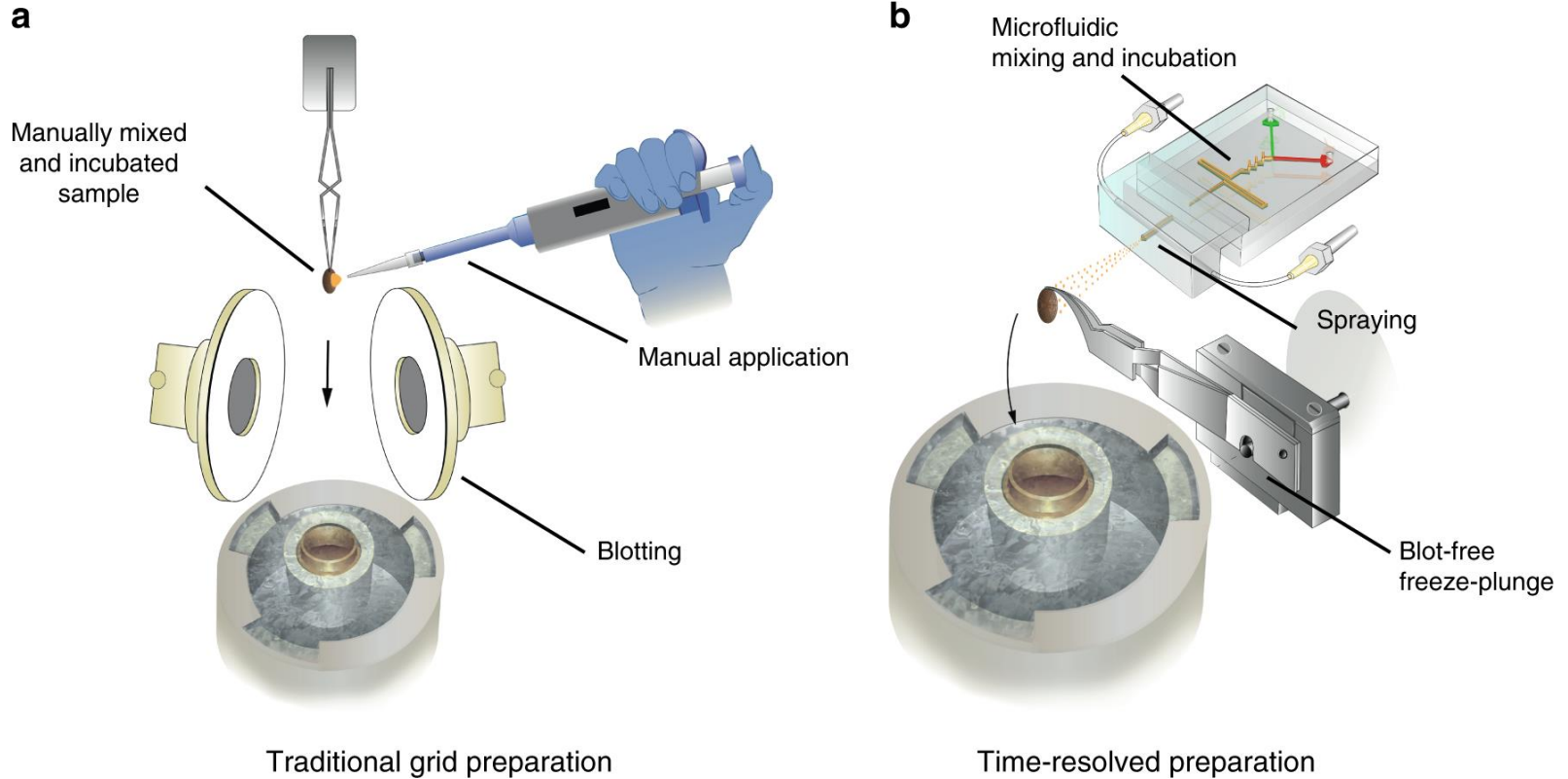


Starting and stopping reactions in real time using a microfluidic chip



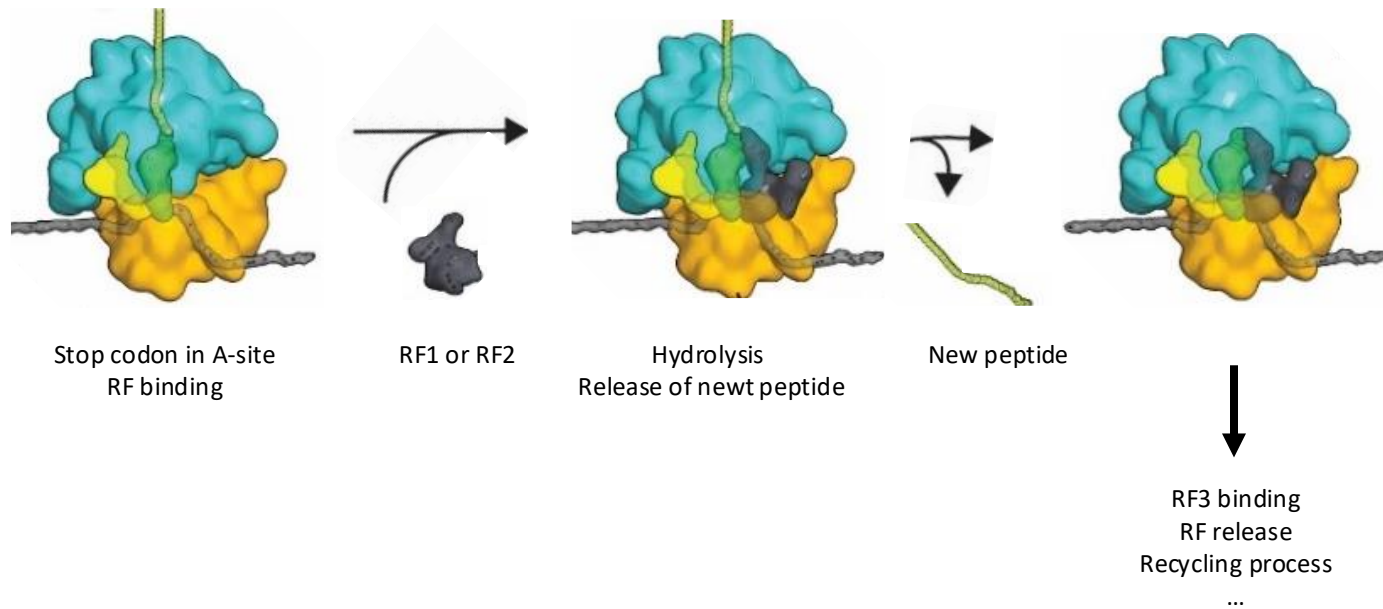
Xiangsong Feng

Time-resolved cryo-EM

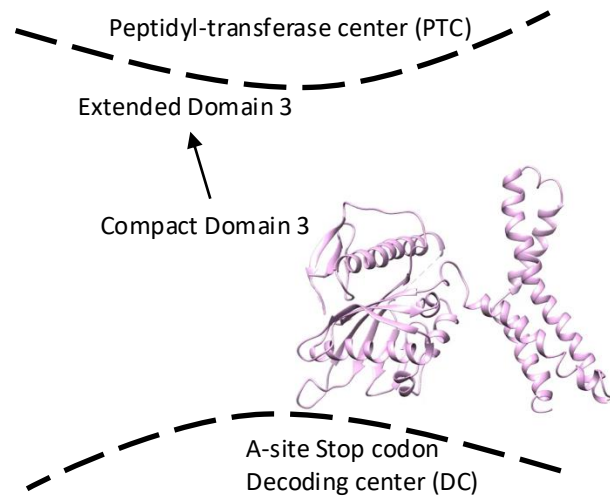


Mäeots et al. Nat. Commun. 2020

Example: translation termination process



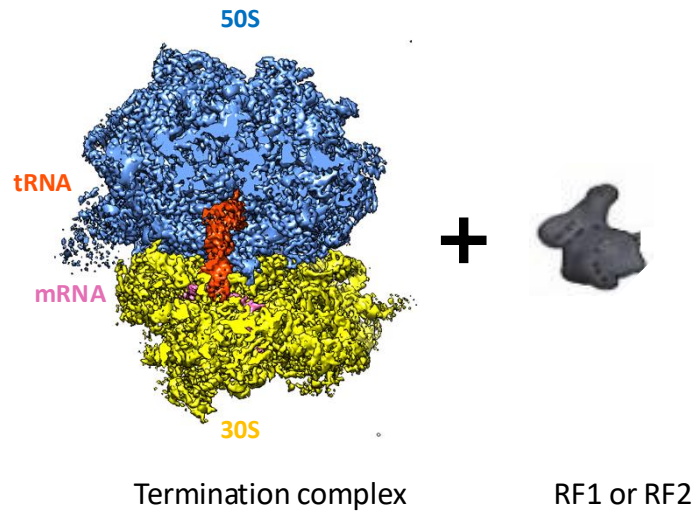
Movie : from compact to extended conformation of RF1



Fu et al.,
Nat. Commun. 2019

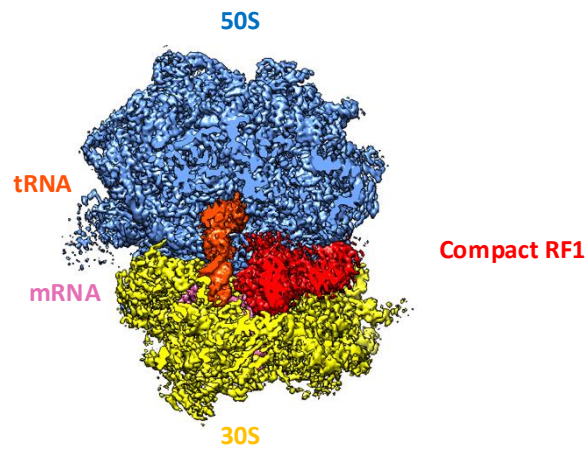
Reactant 1: Termination complex

Reactant 2: RF1 or RF2



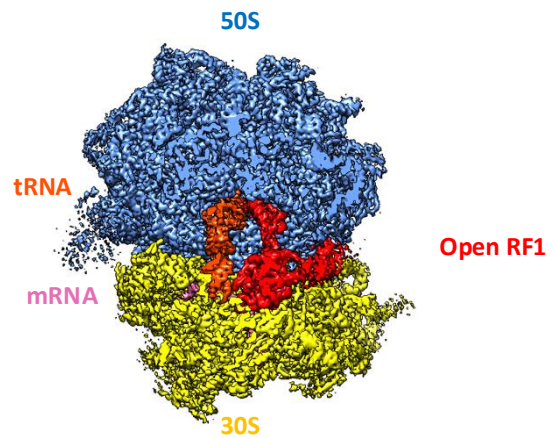
Fu et al.,
Nat. Commun. 2019

RF1 in a compact conformation captured at 24 ms
Pre-accommodated state (intermediate state)



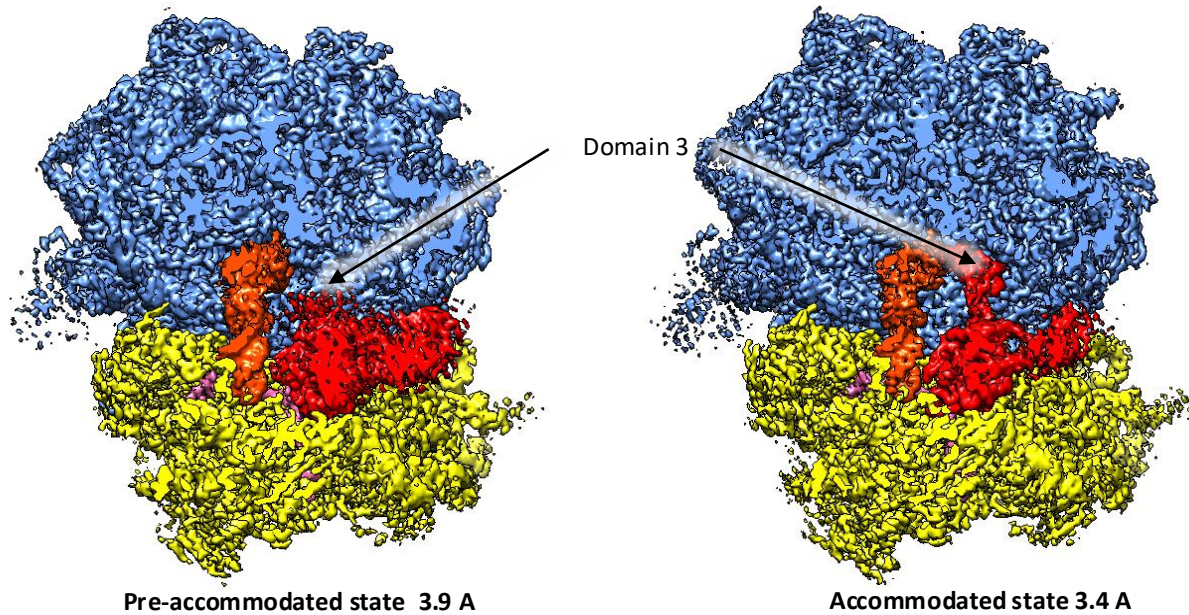
Fu et al.,
Nat. Commun. 2019

RF1 in a extended conformation captured at 60 ms Accommodated state



Fu et al.,
Nat. Commun. 2019

RF1 in pre-accommodated and accommodated states



Fu et al.,
Nat. Commun. 2019

Literature on Time-resolved cryo-EM by Frank Lab:

Applications so far in the bacterial translation field

Shaikh et al., PNAS 2014 – ribosome subunit association

Chen et al., Structure 2015 – ribosome subunit association

Frank, J. Struct. Biol. 2017 – review

Fu et al., Structure 2018 – RRF-mediated ribosome recycling

Kaledhonkar et al., Nature 2019 – translation initiation

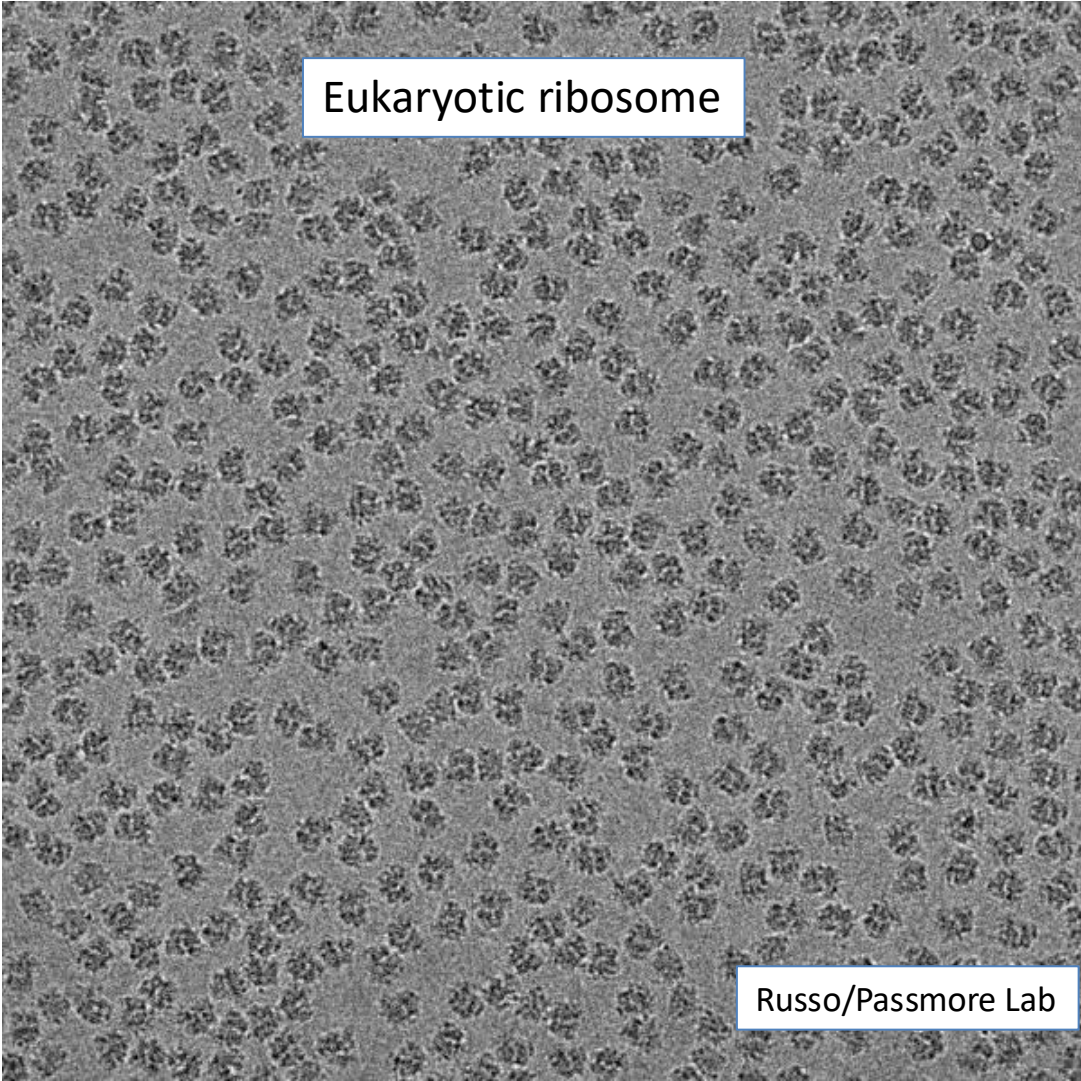
Fu et al., Nature Comm. 2019 – translation termination

Bhattacharjee et al., Cell 2024 – PDMS-based microfluidic chip assembly and HflX-mediated ribosome recycling

Feng and Frank, Bioprotocols 2025 – [a PDMS-based microfluidic chip assembly for time-resolved cryo-EM \(TRCEM\) sample preparation.](#)

Other Labs:

See literature quoted in Bhattacharjee et al., Cell 2024 and Feng & Frank, Bioprotocols 2025

An electron micrograph showing a dense field of small, dark, roughly spherical particles, which are eukaryotic ribosomes. The particles are distributed across the entire frame, appearing as numerous small, dark, irregularly shaped spots against a lighter, grainy background. The overall appearance is that of a highly concentrated population of these cellular organelles.

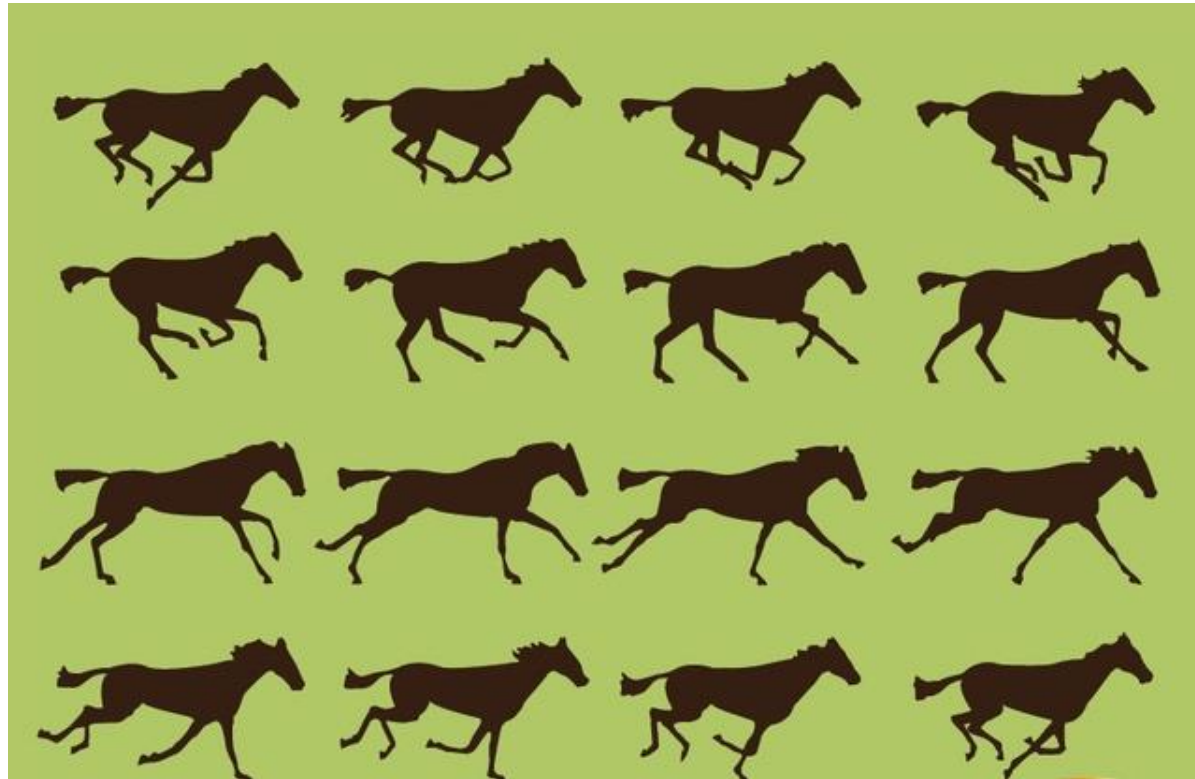
Eukaryotic ribosome

Russo/Passmore Lab



10,000 horses galloping

DO FOR EACH PD of the angular sphere:
order the images sequentially by similarity

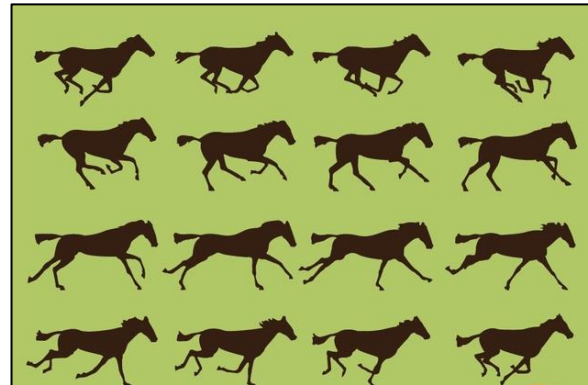


(This is a one-dimensional problem)



By splicing all images from different horses in the sequence of their similarity in forward and backward direction, we get a movie of the average horse galloping

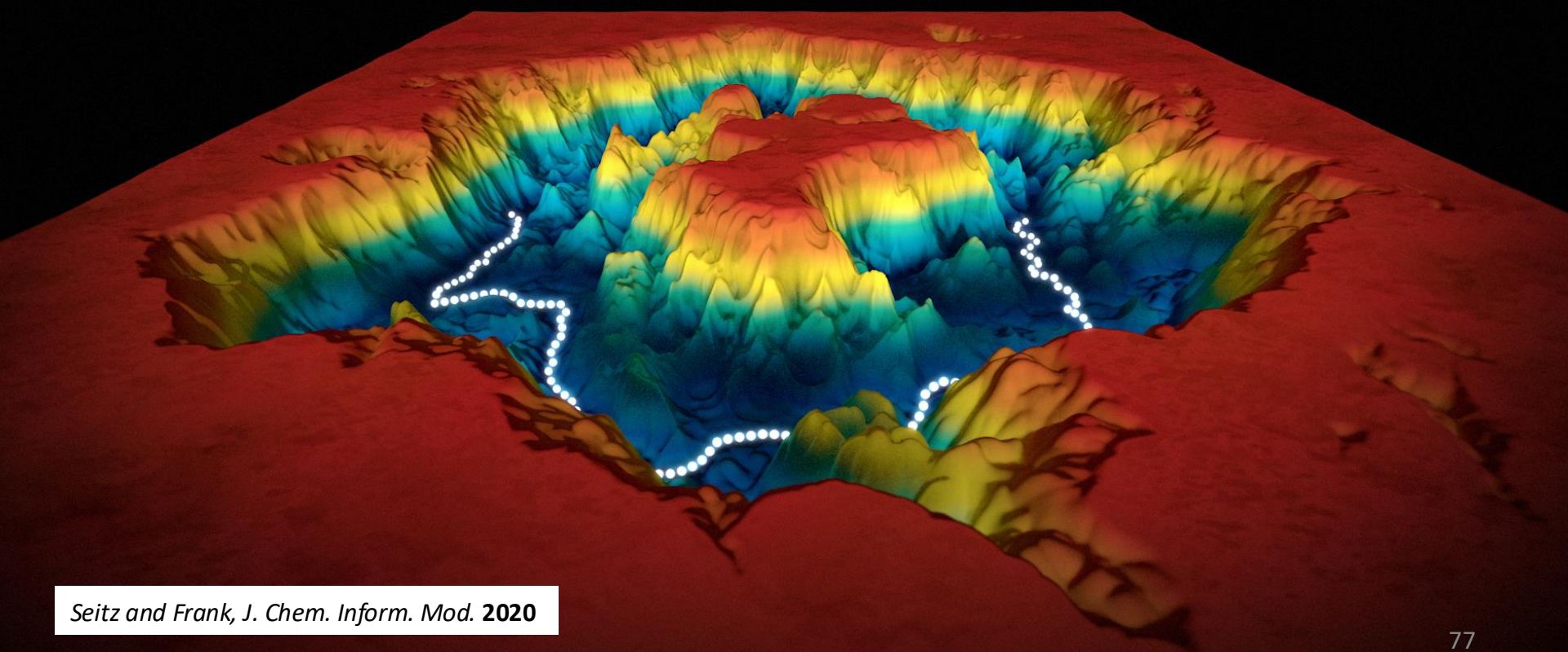
- Reconcile the information from all PDs (Propagation of conformational coordinates across the angular space S^2)
- Next: transform map of occupancies into free energy map.
- Low occupancy \rightarrow high ΔG
- High occupancy \rightarrow low ΔG



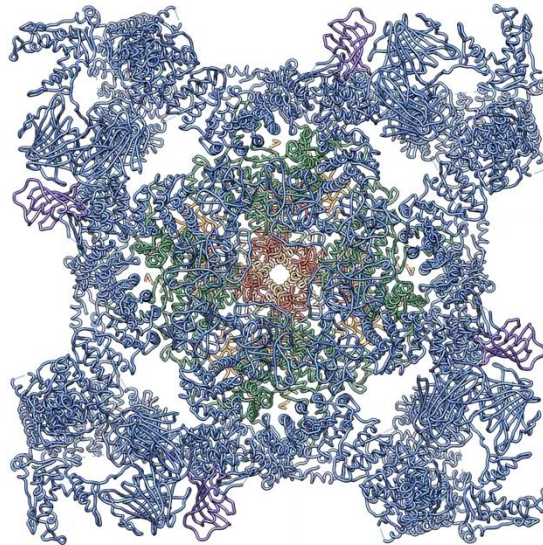
$$\Delta G / k_B T = - \ln (n_c / n_0)$$

Free energy difference Boltzmann const. Temperature No. of mol. in a state No. of mol. in most pop. state

Fischer et al. Nature 2010
 Agirrezabala et al. PNAS 2015



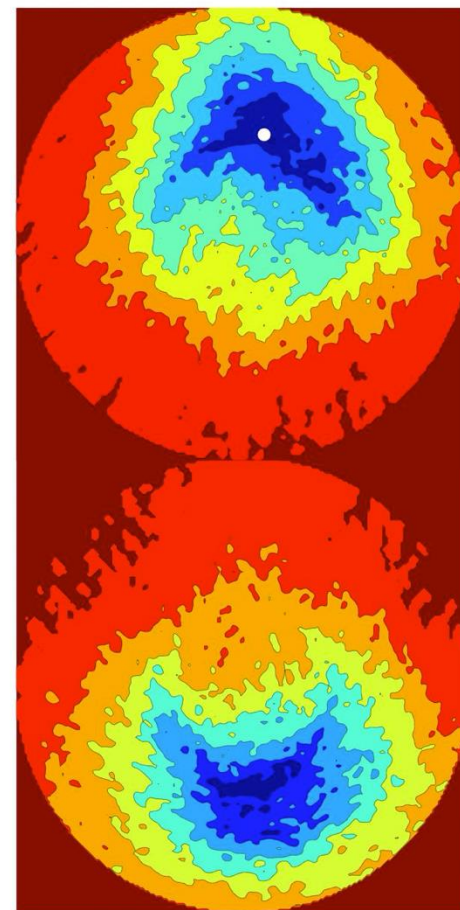
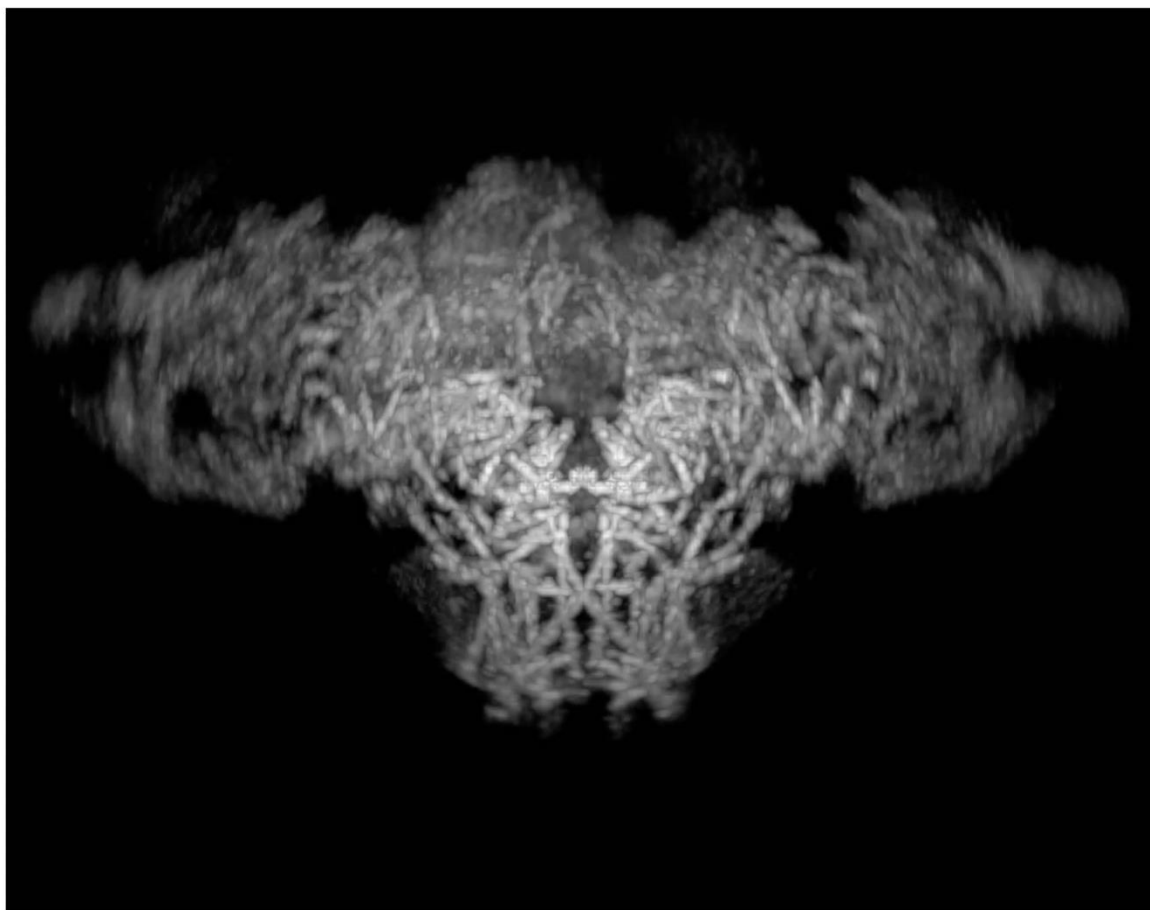
Calcium release channel – Ryanodine receptor



Zalk et al.,
Nature 2016

Marks Lab
Hendrickson Lab
Frank Lab

Des Georges et al., Cell 2017



Dashti et al., Nat. Commun. 2020

Literature on data mining from snapshots of large ensembles of molecules/ Manifold embedding/ ManifoldEM

- Dashti, A. et al. (2014). Trajectories of the ribosome as a Brownian nanomachine. *Proc Natl Acad Sci USA*
- Frank, J., and Ourmazd, A. (2016) Continuous changes in structure mapped by Manifold Embedding of single-particle data in cryo-EM. *Methods* (Review)
- Ourmazd, A. (2019) Cryo-EM, XFELs and the structure conundrum in structural biology. *Nature Meth.* (Review)
- Dashti, A. et al. (2020). Retrieving functional pathways of biomolecules from single-particle snapshots. *Nature Communications*
- Seitz, E., and Frank, J. (2020) POLARIS: Path of Least Action Analysis on Energy Landscapes. *J. Chem. Inf. Model.*
- Maji, S. et al. (2020) Propagation of conformational coordinates across angular space in mapping the continuum of states from cryo-EM data by manifold embedding. *J. Chem. Inf. Model.*
- Sztain, T. et al. (2021). A glycan gate controls opening of the SARS-CoV-2 spike protein. *Nature Chemistry*
- Seitz, E. et al. (2022) Recovery of conformational continuum from single-particle cryo-EM images: Optimization of ManifoldEM informed by ground truth. *IEEE Trans. Comp. Im.*
- Seitz, E. et al. (2023) Beyond ManifoldEM: geometric relationships between manifold embeddings of a continuum of 3D molecular structures and their 2D projections. *Digital Discovery*

Conclusion -- Single-particle cryo-EM: A new era in structural biology

- No need for crystals!
- *Compared to X-ray cryst., very small sample quantity needed*
- Resolution in the 3-4 Å range now routinely achievable
- *Multiple structures retrieved from the same sample → clues on function*
- Molecules in close-to-native conditions
- *Solving structures of membrane proteins much easier than with X-ray crystallography*
- Huge expansion of structural data base relevant for Molecular Medicine



<https://joachimfranklab.org>

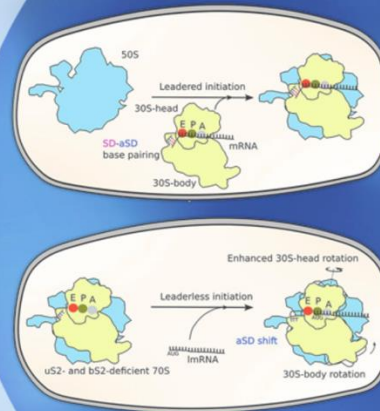


News Blog The Team Research Publications Events Contact Photos Awards

How Dedicated Ribosomes Translate a Leaderless mRNA

Francisco J Acosta-Reyes, Sayan Bhattacharjee, Max Gottesman, Joachim Frank
JOURNAL OF MOLECULAR BIOLOGY

In bacteriophage λ lysogens, the λ cl repressor is encoded by the leaderless transcript (lmRNA) initiated at the λ pRM promoter. Translation is enhanced in *rpsB* mutants deficient in ribosomal protein uS2. Although translation initiation of lmRNA is conserved in bacteria, archaea, and eukaryotes, structural insight of a lmRNA translation initiation complex is missing. Here, we use cryo-EM to solve the structures of the uS2-deficient 70S ribosome of host *E. coli* mutant *rpsB11* and the wild-type 70S complex with λ cl lmRNA and fMet-tRNA^{fMet}. Importantly, the uS2-deficient 70S ribosome also lacks protein bS21. The anti-Shine-Dalgarno (aSD) region is structurally supported by bS21, so that the absence of the latter causes the aSD to divert from the normal mRNA exit pathway, easing the exit of lmRNA. A π -stacking interaction between the monitor base A1493 and A(+4) of lmRNA potentially acts as a recognition signal. Coulomb charge flow, along with peristalsis-like dynamics within the mRNA entrance channel due to the increased 30S head rotation caused by the absence of uS2, are likely to facilitate the propagation of lmRNA through the ribosome. These findings lay the groundwork for future research on the mechanism of translation and the co-evolution of lmRNA and mRNA that includes the emergence of a defined ribosome-binding site of the transcript.



Welcome to Frank Lab

We investigate the mechanism of translation on the ribosome by using cryo-electron microscopy and single-particle reconstruction.



<https://franxfiction.com>



HOME

ABOUT

PUBLISHED

PHOTOGRAPHY

LINKS

CONTACT

FRANX FICTION

I started this website since nowadays one needs a presence to be present, and physical presence is no longer sufficient to be seen in this nebulous virtual space. So think of it as a bullhorn, as an amplification, as a mic check.



END OF LECTURE

The following slides are just some additional
information